TENSILE BEHAVIOR OF ALUMINUM REINFORCED WITH ANGLE-PLY BORON/EPOXY LAMINATES

by

Daniel Ming-Fei Wong

Thesis submitted to the Graduate Faculty of the
Virginia Polytechnic Institute and State University
in partial fulfillment of the requirements for the degree of
MASTER OF SCIENCE
in
Engineering Mechanics

APPROVED:

C. T. Herakovich, Chairman

R. P. McNitt

D. T. Mook

D. Frederick, Department Head

March, 1974

Blacksburg, Virginia

ACKNOWLEDGMENTS

The author is grateful for the support of NASA Langley through NASA Grant NGR-47-004-101 which made this research possible.

The author wishes to thank Dr. Carl T. Herakovich for much guidance and assistance as his major advisor.

He also wishes to acknowledge the help of Messrs. Mike Renieri, Jerald Jones and Chip Wilson in performing the experimental testing program.

He wishes to acknowledge the encouragement of his wife in his pursuit of graduate study.

Finally he thanks Miss Jane Harrison for typing his manuscript.

TABLE OF CONTENTS

LIST OF SYMBOLS

A	Cross sectional area
[A]	inplane stiffness matrix for a laminate
E	modulus of elasticity
F	force
G	shear modulus
h	laminate total thickness
ℓ	length
n	no. of plies
[Q]	lamina stiffness matrix
$[\bar{Q}]$	transformed lamina stiffness matrix
ΔT	temperature change
t	ply thickness
$\{\sigma\}$	stress matrix
$\{\varepsilon\}$	strain matrix
{N}	resultant inplane forces
α	coefficient of thermal expansion
σ^T	residual thermal stress
ν	Poisson's ratio
V	volume fraction

Subscripts

Aℓ	aluminum
B/E	boron/epoxy
k	kth ply

p	proportional limit
y	yield
f	failure
u	ultimate
(ℓ,t)	lamina natural coordinate
(x,y)	arbitrary coordinate system
c	composite

LIST OF FIGURES AND TABLES

Tables Page

1. INTRODUCTION

A composite material is any combination of two or more constituent materials arranged in order to increase their combined structural efficiency. One class of composites known as advanced composites is the combination of high strength, high modulus fibers, embedded in a homogeneous matrix material. Boron and graphite are currently the most popular fibers and epoxy is the most common matrix material.

The search for light weight materials of high strength has been one goal of the aerospace industry for some time. Prior to the advent of composites, aluminum and titanium had been the materials used most often in the industry. These metals were chosen because of their relatively high specific modulus and high specific strength. Specific modulus is the modulus of elasticity of the material divided by its density, and the specific strength is the ultimate stress divided by the density. Since the density of advanced composites is much lower than those of metals, and their modulus and ultimate strength are at least of the same order of magnitude, their specific properties are much superior to those of most metals. Another advantage of composites is that they can be designed not only for the maximum load, as with conventional metals, but also for various directional loading conditions. Hence composites can result in more efficient utilization of material. A considerable amount of effort has been devoted to the investigation of composites for the last decade. Advanced composites such as boron/epoxy and graphite/epoxy have proved to be sound materials for aerospace applications. They have demonstrated weight savings of as much

as 50% in some aerospace components [1]*.

Because composites are anisotropic, analysis of them requires a more general theory than does the analysis of isotropic materials. Constitutive equations and yield or failure criteria must include the directional dependence of the material behavior. The constitutive equations for laminated composites are well known and can be found in any text on the subject [2]. Many failure criteria have been proposed for anisotropic materials. A review of the subject is presented in references [3, 4]. The maximum strain theory [4] is quite simple to use and provides good strength predictions for some laminate configurations. Unfortunately, this theory does not give good results for all configurations. Experimental results have been reported which exhibit strengths well below those predicted by the maximum strain theory [5, 6]. The lower than predicted strengths have often been attributed to edge effects and stacking sequence [7, 8].

A relatively new concept in the application of composites is selective reinforcement of metals with composite laminates. The objective of this concept is to use advanced composites to reinforce conventional metals so as to produce a more efficient and reliable material system. Previous investigations have considered the tensile behavior of metals reinforced with unidirectional boron/epoxy and graphite/epoxy [5, 6]. The results showed that early failures were observed for some co-cured boron/epoxy reinforced aluminum tensile coupons. The strength of these specimens was as much as 62 percent below the predicted values. Other specimens failed at the predicted values. The strength criterion used

* Numbers in brackets [ ] refer to the list of references.

was based on the ultimate strain of the unidirectional composite. It was argued that thermal stresses which resulted form the thermal mismatch of the constituent materials played an important role in initiating the early failures.

The present investigation is a continuation of the research on tensile strength of boron/epoxy reinforced aluminum. This investigation differs from the previous work in that angle-ply composite laminates are considered. The experimental program consisted of two parts: tensile tests on all composite angle-ply specimens and tensile tests on angle-ply composite reinforced aluminum specimens. A theoretical analysis including thermal effects and yielding of the aluminum was also conducted.

2. THEORETICAL CONSIDERATIONS

2.1 Laminate Analysis

Laminated composites generally consist of stacked plies or laminae of continuous unidirectional filaments imbedded in a matrix material. Thus, the individual lamina is the basic building block of a laminated composite. In laminate analysis, the behavior of the individual lamina is assumed to govern the behavior of the laminated composite. An understanding of the individual ply behavior is therefore fundamental to laminate analysis. A lamina may be considered to be a homogeneous orthotropic material. An orthotropic material is a material with different material properties in the three orthogonal principal material directions (Fig. 1a). In laminate analysis, each lamina is assumed to be in plane stress. The general constitutive relationship for a typical lamina in its natural (ℓ,t) coordinate system (along the direction of the fibers and the direction perpendicular to them (Fig. 1b)) is then

$$\begin{Bmatrix} \sigma_\ell \\ \sigma_t \\ \tau_{\ell t} \end{Bmatrix} = \begin{bmatrix} Q_{11} & Q_{12} & Q_{16} \\ Q_{12} & Q_{22} & Q_{26} \\ Q_{16} & Q_{26} & Q_{66} \end{bmatrix} \begin{Bmatrix} \varepsilon_\ell \\ \varepsilon_t \\ \gamma_{\ell t} \end{Bmatrix} \tag{1}$$

where

$$\begin{aligned} Q_{11} &= E_\ell/(1 - \nu_{\ell t}\nu_{t\ell}) \\ Q_{22} &= E_t/(1 - \nu_{\ell t}\nu_{t\ell}) \\ Q_{12} &= E_\ell\nu_{t\ell}/(1 - \nu_{\ell t}\nu_{t\ell}) \\ Q_{66} &= G_{\ell t} \\ Q_{16} &= Q_{26} = 0 \end{aligned} \tag{2}$$

E_ℓ and E_t are the elastic moduli in the fiber direction and transverse to the fibers, respectively; $\nu_{\ell t}$, $\nu_{t\ell}$ are the major and minor Poisson's ratios; $G_{\ell t}$ is the shear modulus. The major Poisson ratio $\nu_{\ell t}$ is defined as the negative ratio of the transverse strain ε_t to an applied longitudinal strain ε_ℓ, thus

$$\nu_{\ell t} = - \frac{\varepsilon_t}{\varepsilon_\ell} \tag{3}$$

The minor Poisson ratio $\nu_{t\ell}$ is accordingly defined

$$\nu_{t\ell} = - \frac{\varepsilon_\ell}{\varepsilon_t} \tag{4}$$

It can easily be shown from the preceding equations that the elastic moduli and Poisson ratios satisfy the relationship

$$E_t \, \nu_{\ell t} = E_\ell \, \nu_{t\ell} \tag{5}$$

The material constants E_ℓ, E_t, $G_{\ell t}$, $\nu_{\ell t}$ and $\nu_{t\ell}$ must be determined experimentally. The matrix of coefficients [Q] is called the lamina stiffness matrix.

For a lamina with the fibers aligned at some angle θ to the reference axes x, y (Fig. 1c), the stress-strain relationship can be expressed in terms of the transformed stiffness matrix $[\bar{Q}]$

$$\begin{Bmatrix} \sigma_x \\ \sigma_y \\ \tau_{xy} \end{Bmatrix} = \begin{bmatrix} \bar{Q}_{11} & \bar{Q}_{12} & \bar{Q}_{16} \\ \bar{Q}_{12} & \bar{Q}_{22} & \bar{Q}_{26} \\ \bar{Q}_{16} & \bar{Q}_{26} & \bar{Q}_{66} \end{bmatrix} \begin{Bmatrix} \varepsilon_x \\ \varepsilon_y \\ \gamma_{xy} \end{Bmatrix} \tag{6}$$

The state of stress $\{\sigma\}_k$ in the $k^{\underline{th}}$ ply of a laminate may be expressed in contracted notation as

$$\{\sigma\}_k = [\bar{Q}]_k \, \{\varepsilon\}_k \tag{7}$$

For a laminate which is symmetric with respect to the middle plane, the in-plane forces per unit length $\{N\} = \begin{Bmatrix} N_x \\ N_y \\ N_{xy} \end{Bmatrix}$ (Fig. 2) are expressed in terms of the midplane strains $\{\varepsilon\}$ as

$$\{N\} = [A]\{\varepsilon\} \tag{8}$$

where

$$[A] = \sum_{k=1}^{n} [\bar{Q}]_k (h_k - h_{k-1}) \tag{9}$$

and h_k is the distance from the bottom of the kth ply to the middle surface as shown in Fig. 2 and n is the total number of plies in the laminate. The average laminate stresses $\{\sigma\}$ are then

$$\{\sigma\} = \frac{1}{h}\{N\} \tag{10}$$

where h is the total laminate thickness. If [a] is defined

$$[a] = \frac{1}{h}[A] \tag{11}$$

then

$$\{\varepsilon\} = [a]^{-1}\{\sigma\} \tag{12}$$

The elastic modulus E_x of a laminate subjected to axial loading σ_x is then

$$E_x = \frac{\sigma_x}{\varepsilon_x} = \frac{1}{[a_{11}]^{-1}} \tag{13}$$

Thus, for a symmetric specially orthotropic laminate with constant ply thickness t, the modulus in the loading direction, as predicted by laminate theory, is

$$E_x = \frac{t}{h}\left\{ \sum_{k=1}^{n} (\bar{Q}_{11})_k - \frac{\left[\sum_{k=1}^{n} (\bar{Q}_{12})_k\right]^2}{\sum_{k=1}^{n} (\bar{Q}_{22})_k} \right\} \tag{14}$$

Equation (14) is valid for isotropic as well as orthotropic layers.

The analysis presented here does not include bending-stretching coupling since all laminates used in the experimental program were symmetric.

2.2 Rule of Mixtures

A very simple analytical approach for determining the longitudinal modulus of a composite laminate is known as the rule of mixtures. If a load is applied along the axis of a specimen, each individual constituent of a composite may be assumed to undergo the same axial strain ε. In the elastic range, the stresses in each constituent are then

$$\begin{aligned} \sigma_1 &= E_1 \varepsilon \\ \sigma_2 &= E_2 \varepsilon \end{aligned} \tag{15}$$

where the subscripts 1 and 2 refer to the two constituents. The total cross sectional area A consists of the areas of both constituents:

$$A = A_1 + A_2$$

The total force F on the composite is then

$$F = \sigma A = \sigma_1 A_1 + \sigma_2 A_2 = E_1 A_1 \varepsilon + E_2 A_2 \varepsilon \tag{16}$$

from which the composite modulus E is

$$E = \frac{\sigma}{\varepsilon} = \frac{E_1 A_1}{A} + \frac{E_2 A_2}{A} \tag{17}$$

Denoting the volume fractions of the constituents by V_1 and V_2, Equation (17) becomes

$$E = E_1 V_1 + E_2 V_2 \tag{18}$$

Equation (18) is the rule of mixtures; it can be extended to more than two constituent materials. The rule of mixtures is simply to apply when the modulus and volume fraction of each constituent material are

known. It has been shown to be quite accurate in predicting the modulus in the fiber direction but, in general, does not give good results for other loading directions.

2.3 Laminate Thermal Analysis

Most materials expand or contract when exposed to temperature changes. If the solid is homogeneous and isotropic, it either expands or contracts the same amount in all directions as a function of the temperature change ΔT. Because composites are anisotropic, the coefficient of thermal expansion is different in different directions. An individual composite lamina has two principal coefficients of thermal expansion: one in the direction parallel to fibers and the other in the directions perpendicular to the fibers. For a single ply of arbitrary orientation θ, the coefficients of thermal expansion, α_x, α_y, α_{xy} (Fig. 1c) are governed by the transformation equations:

$$\left.\begin{aligned} \alpha_x &= \alpha_\ell \cos^2\theta + \alpha_t \sin^2\theta \\ \alpha_y &= \alpha_\ell \sin^2\theta + \alpha_t \cos^2\theta \\ \alpha_{xy} &= 2\cos\theta \sin\theta\, \alpha_\ell - 2\cos\theta \sin\theta\, \alpha_t \end{aligned}\right\} \qquad (19)$$

where α_ℓ, α_t are the longitudinal and transverse coefficients of thermal expansion in the lamina natural coordinate system.

In composite reinforced metals, there may be a large thermal mismatch between the composite and the metal depending on the lay-up configuration. (Table 1 shows the thermal properties of each of the constituent materials used in this investigation.) The test specimens to be investigated were co-cured at a high temperature (350°F) and then were cooled to room temperature. This fabrication process is

advantageous for high temperature applications. However, as the result of the change in temperature during cooling, residual thermal stresses are developed in each constituent material or lamina.

Consider a symmetric laminate consisting of three distinct plies each having different coefficients of thermal expansion. The laminae are bonded together at a high temperature and subsequently cooled to room temperature. Thermal stresses are introduced because the individual plies of the laminate are constrained from contracting to their free length after becoming bonded at the high temperature. During the cooling period, there are no lateral constraints on the laminate; hence, the internal forces F_1, F_2 and F_3 (Fig. 3), must sum to zero

$$F_1 + F_2 + F_3 = 0 \tag{20}$$

In terms of thermal stresses σ^T, equation (20) is

$$\sigma_1^T V_1 + \sigma_2^T V_2 + \sigma_3^T V_3 = 0 \tag{21}$$

Due to the symmetry of the laminate, the panel remains flat and, at some small distance from the free edges, the internal stresses σ_1^T, σ_2^T and σ_3^T become uniform over the thickness of each ply. Assuming the deformation to be elastic, the one-dimensional stress-strain equation for each material is written

$$\left.\begin{aligned} \varepsilon_1 &= \alpha_1 \Delta T + \frac{\sigma_1^T}{E_1} \\ \varepsilon_2 &= \alpha_2 \Delta T + \frac{\sigma_2^T}{E_2} \\ \varepsilon_3 &= \alpha_3 \Delta T + \frac{\sigma_3^T}{E_3} \end{aligned}\right\} \tag{22}$$

The three plies undergo the same total strain

$$\varepsilon = \frac{\delta}{\ell} = \varepsilon_1 = \varepsilon_2 = \varepsilon_3 \tag{23}$$

where δ is the change in length of the laminate and ℓ is its original length. (The difference between changes in length prior to bonding is neglected.) From the above equations, the residual thermal stresses for each ply are

$$\sigma_1^T = E_1 \Delta T \left\{ \frac{(\alpha_2 - \alpha_1)E_2V_2 + (\alpha_3 - \alpha_1)E_3V_3}{E_1V_1 + E_2V_2 + E_3V_3} \right\} \tag{24}$$

$$\sigma_2^T = E_2 \Delta T \left\{ \frac{(\alpha_1 - \alpha_2)E_1V_1 + (\alpha_3 - \alpha_2)E_3V_3}{E_1V_1 + E_2V_2 + E_3V_3} \right\} \tag{25}$$

$$\sigma_3^T = E_3 \Delta T \left\{ \frac{(\alpha_1 - \alpha_3)E_1V_1 + (\alpha_2 - \alpha_3)E_2V_2}{E_1V_1 + E_2V_2 + E_3V_3} \right\} \tag{26}$$

Equations (24 - 26) may be extended to any number of layers.

These equations are approximate since a one-dimensional analysis has been used. However, limited results using a finite element approach [6] showed that they do give a reasonable approximation away from the edges.

2.4 Failure Criteria

Various failure criteria have been proposed for anisotropic materials such as filamentary composites [3, 4, 9]. Due to the complexity of the distinct modes of failure of composites, a simple failure criterion is not available. Failure of composites may involve fiber breakage, matrix cracking and/or debonding. The validity of any criterion can only be verified by experimental results.

The failure criterion used in the present theoretical analysis is the maximum principal strain theory [4]. For orthotropic material under plane

stress, this theory assumes that failure occurs whenever any principal strain attains its maximum value, i.e.,

$$\begin{aligned} \varepsilon_{\ell} &= \varepsilon_{\ell_{max}} \\ \varepsilon_{t} &= \varepsilon_{t_{max}} \\ \gamma_{\ell t} &= \gamma_{\ell t_{max}} \end{aligned} \tag{27}$$

These maximum values can be obtained from tension tests in the fiber and transverse directions and a pure shear test. This theory is relatively easy to apply for analysis. It gives good results for some laminates but it is not generally applicable to angle-ply composite laminates [6].

2.4.1 All Composite Laminates

For the angle-ply composite laminates, failure is assumed to occur whenever a principal strain in any lamina equals its ultimate or maximum value. Residual thermal strains must also be included for a complete analysis. For an arbitrary ply of orientation θ, the strain in its natural coordinate system is obtained from the transformation equation

$$\begin{Bmatrix} \varepsilon_{\ell} \\ \varepsilon_{t} \\ \frac{1}{2}\gamma_{\ell t} \end{Bmatrix} = [T] \begin{Bmatrix} \varepsilon_{x} \\ \varepsilon_{y} \\ \frac{1}{2}\gamma_{xy} \end{Bmatrix} \tag{28}$$

where [T] is the transformation matrix

$$[T] = \begin{bmatrix} \cos^2\theta & \sin^2\theta & 2\sin\theta\cos\theta \\ \sin^2\theta & \cos^2\theta & -2\sin\theta\cos\theta \\ -\sin\theta\cos\theta & \sin\theta\cos\theta & (\cos^2\theta - \sin^2\theta) \end{bmatrix} \tag{29}$$

For laminates consisting of an equal number of 0° and 90° plies, failure is assumed to occur at the ultimate strain of the 0° plies. The contribution of the 90° plies to the strength of the laminate is negligible. These 90° plies are therefore neglected in the ultimate strength analysis. However, failure of the 90° plies will cause nonlinearity in the stress-strain behavior of the laminate. The failure stress σ_f can be written

$$\sigma_f = VE(\varepsilon_u - \varepsilon^T) \tag{30}$$

where V and E are the volume fraction and modulus of the 0° plies in a laminate and ε_u and ε^T are the ultimate strain measured from the stress free state and the residual thermal strain of the 0° plies, respectively. Equation (30) can be simply written in terms of the failure strain ε_f, which is the strain that must be applied to reach failure starting from a residual state,

$$\sigma_f = VE\ \varepsilon_f \tag{31}$$

where

$$\varepsilon_f = \varepsilon_u - \varepsilon^T \tag{32}$$

For other laminate configurations, strains are transformed to the natural coordinate system (eqn. 28) and failure is then predicted by equation (27).

2.4.2 Composite Reinforced Aluminum Laminates

For this material system, failure of the laminate is assumed to occur at the ultimate strain of the composite system as predicted in the previous section.

For bidirectional (0° and 90°) composite reinforced aluminum panels,

the 90° plies are assumed to fail early and are neglected in the strength analysis. Treating the aluminum to be an elastic, linear hardening material with modulus $E_{A\ell}$ and strain hardening parameter m, the failure stress for the laminate is

$$\sigma_f = VE\ \varepsilon_f + V_{A\ell} E_{A\ell}[(1 - m)(\varepsilon_{A\ell}{}^{y} - \varepsilon_{A\ell}{}^{T}) + m\varepsilon_f] \qquad (33)$$

where $\varepsilon_{A\ell}{}^{y}$ is the yield strain of aluminum and $\varepsilon_{A\ell}{}^{T}$ is the residual thermal strain of aluminum and $V_{A\ell}$ is the volume fraction of aluminum in the laminate.

For other panel configurations, strains are transformed to the natural coordinate system. Then the maximum strain theory is used to predict the failure strain and stress.

2.5 Interlaminar Stress Effects

When a composite laminate is composed of layers of different orientations or different materials, interlaminar stresses are developed at the laminae interfaces because of the mechanical and thermal mismatch between laminae. Laminate theory considers these stresses to be higher order effects. Laminate theory also ignores the zero boundary condition along free edges. Numerical analysis shows that these interlaminar stresses are significant near the free edges of a coupon laminate [10]. Laminate theory can only predict the in-plane stresses away from the edges. An understanding of the shear and normal stress transfer mechanism between layers of the composites is believed to be important in analyzing the early failures of some laminates. Figure 2 shows the geometry of a laminate and the stress components acting on a typical element. For a bidirectional laminate (0° and 90° plies) the interlaminar normal stress σ_z may be the most important factor influencing

the strength of the laminate [11]. Figure 4 shows the direction of the interlaminar stress components acting on the 0° ply of a symmetric $[0/90]_s$ laminate. From laminate theory and residual thermal stress analysis, tensile normal stress σ_y is developed in the 0° ply and compressive normal stress σ_y is developed in the 90° ply under a tensile loading σ_x. For equilibrium in the y direction and moment equilibrium about the x axis, the equilibrium equations are

$$\sum F_y = 0$$

$$h_0 \sigma_y = \int \tau_{zy} \, dy \tag{34}$$

$$\sum M_x = 0$$

$$h_0^2 \sigma_y/2 = \int y \, \sigma_z \, dy \tag{35}$$

where h_0 is the ply thickness. Hence a tensile interlaminar normal stress σ_z is developed near the edge of the interface for this stacking sequence. If the stacking sequence is reversed, the laminate geometry becomes $[90/0]_s$ and σ_y in the upper (90°) layer is now compressive. From the above equilibrium conditions the interlaminar normal stress σ_z along the interface will now be compressive. It is believed that tensile σ_z leads to debonding and hence a weaker laminate than that with a compressive σ_z.

3. EXPERIMENTAL PROGRAM

3.1 Test Specimen

Two groups of coupon tensile specimens were tested during the course of this investigation. One group was composite angle-ply boron/epoxy laminates (Narmco 5505/4) and the other group was angle-ply boron/epoxy reinforced aluminum laminates [7075-T6-Aℓ]. The latter group had aluminum sandwiched between symmetric boron/epoxy laminates (Fig. 5). Both groups of coupon specimen were symmetric with respect to the mid-plane. All specimens were the standard IITRI coupon and nominally measured 12 inches in length and 0.5 inches in width. The total thickness varied with the number of plies of boron/epoxy in each laminate. All the laminates were laid up from rolls of 3 inch wide prepeg tape. After the desired configuration was laid up, large panels were co-cured at 350°F in an autoclave according to manufacturer's specifications and then cooled to room temperature. No adhesives were used to bond the composite to the metal. The epoxy resin acted as the bonding agent for all specimens. The laminates were then machine cut to the final shape of the coupon specimen. Tapered 2.5 inches by 0.5 inches fiber glass tabs were bonded to the specimen ends for gripping leaving 7 inches of free gage length. The tabs were bonded with contact cement (Aron Alpha). Typical specimen dimensions are also shown in Fig. 5 and a picture of a specimen is shown in Fig. 6. All specimens were fabricated at NASA Langley. There were no difficulties encountered when bonding the boron/epoxy to the aluminum. A complete list of specimen configurations is presented in Table 2.

3.2 Test Procedure

The experimental testing of the specimens was performed at VPI&SU on a 20,000 pound capacity Instron Testing Machine. Each specimen was loaded in tension to failure. The load was transferred to the specimen through standard friction grips under constant head rate. A load-time data output was obtained from the strip chart on the Instron Machine. Four electrical resistance foil type strain gages were mounted on each specimen for measurement of strain. Two gages were axially bonded and the other two transversely (Fig. 6). The use of two gages on each face of the specimen was necessary to check for bending and to insure reliability of the data obtained. No significant bending was encountered during the testing program. The data presented here is the average of the two gages. The strains were usually recorded with a Brown Engineering 251 Multi-Channeled Data Acquisition System (10,000 μ in./in. strain capacity). Strain-time output was generated in digital form using this system. For strains over 10,000 μ in./in., such as would be expected in the ±45° specimens, four Vishay Bridge Amplifier Meter units and two strip chart recorders were used. Some tests were run using both recording systems as a cross-check. Good agreement of strain readings between both systems was obtained. Stresses were calculated based on the average initial cross sectional area of each specimen. A stress-strain curve for each specimen was then constructed from the strain-time and stress-time curves. At least two specimens of each lay-up configuration were tested. A third specimen was tested if the results of the first two tests showed any appreciable difference. Table 3 lists all results

for the specimens tested in this program.

Acoustic emissions from the specimens were also recorded during the tests. The acoustic emission data have been recorded on tape and will be analyzed as part of a related investigation. Figures 7 & 8 show the experimental set up and aparatus used in this investigation.

4. RESULTS AND DISCUSSIONS

4.1 Introduction

A complete listing of all results obtained in this investigation is presented in Table 3. Average values for each specimen configuration are given in Table 4 and typical experimental results for stress-strain behavior are compared to the theoretical curves in Figures 9 to 20.

The residual thermal stresses in Table 4 are obtained from equations (24) to (26). The residual thermal strains are the corresponding elastic strains. The total strain in each ply of different material or fiber orientation is the algebraic sum of the residual strain and the measured strain due to the applied load. The total stress is the stress corresponding to the total strain on the stress-strain curve. The actual failure stress is the ultimate applied load divided by the average cross-sectional area of the specimen. The theoretical failure stress is calculated based on the maximum strain of the composite and the predicted residual thermal strain (Eqn. 30 to 33). Experimentally determined moduli and average Poisson ratios are compared with predicted values in Table 5.

4.2 Composite Laminates

4.2.1 [0] Laminates

Figure 9 presents typical stress-strain behavior for unidirectional [0] boron/epoxy. The curve is linear up to failure. As shown in Table 5 the average modulus of elasticity for all tests was 26.7×10^6 psi. The average ultimate stress and ultimate strain for these specimens were 213.0 ksi and 8,070 μ in/in, respectively. These values were used for predicting the behavior of all other laminates which had one or more 0° plies. The transverse strain is also presented as a function of stress in this figure.

It is also a linear curve and, therefore, the major Poisson ratio $\nu_{\ell t}$ is constant throughout the total strain range. The average value of $\nu_{\ell t}$ for all tests was 0.22.

4.2.2 [90] Laminates

Figure 10 shows typical stress-strain behavior for the transverse [90] laminates. The curve is linear up to a strain of approximately 2,400 μ in/in and then nonlinear to failure at a strain of 3,225 μ in/in. The average experimentally determined elastic modulus was 2.53×10^6 psi and the average ultimate stress was 7.55 ksi (Table 4). The strength data obtained were low compared with that obtained from reference [12]. The results presented in reference [12] were 9.3 ksi and 4,300 μ in/in for the ultimate stress and strain, respectively. For the theoretical analysis of the present investigation, an ultimate stress of 9.0 ksi, an ultimate strain of 4,000 μ in/in and an elastic modulus of 2.53×10^6 psi were used.

Transverse strain was also recorded during these tests. The maximum transverse strain obtained was 50 μ in/in. The average Poisson ratio $\nu_{t\ell}$ was 0.02 for this laminate.

4.2.3 [±45] Laminates

Stress-strain behavior of the $[45_2/\text{-}45_2]_s$ laminate is shown in Figure 11. The results obtained were typical for this type of laminate. The figure shows that longitudinal and transverse strains exhibit very similar behavior. The curves also show early nonlinearity. An initial elastic modulus was determined to be 3.2×10^6 psi. The average ultimate axial strain was 16,000 μ in/in. The Poisson ratio ν_{xy} was essentially constant at a value of 0.85. The ultimate stress was 17.2 ksi. The data obtained in this investigation compared very well with the experimental results presented in reference [12].

4.2.4 [0/90] Bidirectional Laminates

There were three configurations for this type of laminate: $[0_3/90]_s$, $[0_2/90_2]_s$ and $[90_2/0_2]_s$. Typical stress-strain diagrams for the three laminates are compared to the theoretical curves in Figures 12 and 13.

Three specimens of the $[0_3/90]_s$ configuration were tested. The results were not entirely consistent. As shown in Table 3, the experimentally determined moduli were 19.5 x 10^6 psi, 20.0 x 10^6 psi and 21.0 x 10^6 psi while the predicted value is 20.7 x 10^6 psi. The stress-strain behavior for two of the three laminates was nearly linear to failure. The ultimate stresses obtained for these two specimens were 146.0 ksi and 126.0 ksi and the failure strains were 7,800 μ in/in and 6,800 μ in/in, respectively. The predicted values based on the failure of the 0° plies were 163.0 ksi and 8,193 μ in/in. The third specimen exhibited a rather distinct knee at a strain of 1,200 μ in/in. This specimen with the bilinear behavior failed much earlier than the other two specimens. The ultimate stress and strain obtained were 108.0 ksi and 6,400 μ in/in, respectively.

One possible explanation for the lower than predicted failures is that they are due to extensive fiber breakage and/or debonding which are initiated by the failure of the 90° plies. Fiber breakage would be indicated by a decrease in modulus. The first two specimens, which exhibited nearly linear behavior, both had a final modulus prior to failure of 18.0 x 10^6 psi. This compares fairly well with the predicted value of 20.0 x 10^6 psi which is based upon zero

stiffness contribution from the 90° plies. The third specimen had a final modulus of 16.5 x 10^6 psi indicating more extensive fiber breakage. It also had the lowest ultimate stress. The average data for all the tests are presented in Table 4. In general, they indicate that the initial elastic modulus agrees with the predicted value. The ultimate strain is below the ultimate strain of the 0° plies, but is above that of the 90° plies. The ultimate stresses are also compared to the predicted values from the Point Stress Laminate Analysis Program SQ5[13] in Table 6. SQ5 is only a linear analysis program and residual thermal stresses are not included in the analysis. The failure stress is based on the maximum strain theory (Eqn. 27). From the SQ5 laminate analysis program, the predicted ultimate strength is 82.8 ksi. This does not compare well with the experimental value because in addition to the limitations stated above the program also neglects the fact that load may be carried by the remaining 0° plies after failure of the 90° plies.

The transverse strain was very small in comparison to the axial strain and hence was not shown on the figure. The average Poisson ratio ν_{xy} was 0.07 compared to the predicted value of 0.062.

For the other two types of bidirectional laminates, the average experimentally determined moduli were 15.5 x 10^6 psi for the $[0_2/90_2]_s$ and 13.5 x 10^6 psi for the $[90_2/0_2]_s$ laminate. From laminate theory the predicted modulus for both configurations is 14.6 x 10^6psi. Thus the elastic modulus for the $[0_2/90_2]_s$ laminate was slightly higher than the predicted value while reversing the stacking sequence

to $[90_2/0_2]_s$ resulted in a modulus which was slightly lower than predicted (As can be seen in Table 3 this was true for all specimens tested). One possible explanation for the lower modulus with the 90° plies on the outside is that some damage had occurred in the outer plies.

The stress-strain diagrams were basically bilinear for both configurations except for one specimen of the $[90_2/0_2]_s$ laminate. This laminate exhibited no distinct knee, failed at a stress of 70.0 ksi and a strain of 6,300 μ in/in. These were the highest values obtained and indicated that less extensive fiber breakage had occurred for this specimen. For the $[0_2/90_2]_s$ laminates, the knee occurred at a strain of 1,350 μ in/in while it occurred at a strain of 1,500 μ in/in for the $[90_2/0_2]_s$ laminates. The expected knees, based upon failure of the 90° plies, were predicted to occur at a strain of 440 μ in/in for both configurations with residual thermal strains included. The expermental results indicate that the thermal strains were lower than predicted.

Comparing these two types of laminates with reversed stacking sequence, the $[90_2/0_2]_s$ laminates were stronger than the $[0_2/90_2]_s$ laminates. The ultimate stresses obtained for the $[90_2/0_2]_s$ laminates were 15% to 35% higher than those of the $[0_2/90_2]_s$ laminates (Table 3). Such behavior could be explained by the presence of compressive interlaminar normal stress σ_z near the edges of the $[90_2/0_2]_s$ laminates (Sect. 2.5). The tensile interlaminar normal stress σ_z for the $[0_2/90_2]_s$ laminates may lead to debonding and early failure. For the $[0_2/90_2]$ laminates, the average ultimate stress and strain were

36.5 ksi and 3,450 μ in/in, respectively. For the $[90_2/0_2]_s$ laminates, results were rather varied. Ultimate stresses obtained were 70.0 ksi, 42.0 ksi and 58.0 ksi (56.7 average) and ultimate strains were 6,300 μ in/in, 4,400 μ in/in and 6,000 μ in/in (5567 average). The predicted values, based on the failure of the 0° plies, were 112.0 ksi for the ultimate stress and 8,417 μ in/in for the ultimate strain for both configurations. From SQ5, the predicted failure stress is 58.6 ksi which is based on the failure of the 90° plies not including thermal stresses. This value is in the range of ultimate stress obtained for the $[90_2/0_2]_s$ laminate but well above the data obtained for the $[0_2/90_2]_s$ laminate. Early failure of these laminates is believed to be mainly due to extensive fiber breakage and/or debonding which is initiated by the rupture of the 90° plies.

The transverse strains were very small in comparison to the axial strains and hence, are not shown in the figure. The average Poisson ratios ν_{xy} were 0.04 and 0.03 for the $[0_2/90_2]_s$ and the $[90_2/0_2]_s$ laminates, respectively. These values compare well with the predicted value of 0.036.

4.2.5 $[45_2/-45_2/90]_s$ Laminates

The last configuration for the all composite specimens is the $[45_2/-45_2/90]_s$ laminate. The stress-strain diagram for this panel is compared to the theoretical curve in Figure 14. Two specimens were tested and the results were consistent (Table 3). Both specimens exhibited an initial linear curve followed by a gradual nonlinearity to failure. The proportional limit was at a strain of 2,300 μ in/in

for both specimens. The average experimentally determined modulus was 4.65×10^6 which agreed quite well with the predicted value of 4.9×10^6 psi. From the residual thermal stress analysis, the 90° plies were in residual tension with a residual tensile strain of 1,700 μ in/in while the ±45° plies were in residual compression. Based on the failure of the 90° plies at a strain of 4,000 μ in/in, the laminate is expected to exhibit a knee at an applied strain of 2,300 μ in/in. However, the proportional limit may be due to failure of the 90° plies and/or nonlinearity of the ±45° plies. The SQ5 laminate analysis program predicts the failure stress to be 19.6 ksi which agrees well with the experimental failure stress of 19.0 ksi. This indicates some contribution to the ultimate stress from the 90° plies; therefore the first nonlinearity does not appear to correspond to failure of the 90° plies. As shown in Figure 14 the experimental ultimate stress is higher than the predicted value of 13.0 ksi based on the sum, through the thickness, of the stress contribution from each layer. The average ultimate strain obtained was 4,850 μ in/in which is far below the ultimate strain of the ±45° laminate but is higher than that of the all 90° laminate. The failure of the laminate is believed to be due to rupture of the 90° plies coupled with interlaminar and edge effects. The ultimate stress obtained is higher than either the $[45_2/-45_2]$ laminate or the [90] laminate.

The transverse strain is also presented in the figure as a function of stress. It exhibited behavior similar to the axial strain. The Poisson ratio ν_{xy} is essentially constant and the value was determined to be 0.45 which is also the predicted value.

4.3 Composite Reinforced Aluminum Laminates

4.3.1 7075-T6 Aluminum Alloy

Figure 9 shows typical stress-strain behavior for 7075-T6 aluminum alloy. It has a modulus of elasticity of 10.0×10^6 psi and the proportional limit is at a strain of approximately 4,500 μ in/in. A yield stress of 52.0 ksi and a yield strain of 5,200 μ in/in were used in the analysis. For the strength analysis, the aluminum alloy is assumed to be an elastic, linear strain-hardening material with strain-hardening parameter m = 0.05 (m is defined as the ratio of the slope of the strain-hardening portion of the stress-strain curve to the elastic modulus).

4.3.2 [O/Aℓ] Laminates

Figure 15 presents the theoretical and experimental stress-strain diagrams for aluminum reinforced with unidirectional (0°) composite, $[0_4/A\ell]_s$ ($V_c = 0.50$). The modulus of elasticity agreed well with the predicted value of 18.4×10^6 psi as the experimental value was 18.75×10^6 psi. The results also agreed with data presented in references [6, 7]. The experimentally determined curve was bilinear. A very distinct knee occurred at a strain of approximately 2,000 μ in/in. From laminate thermal stress analysis, the aluminum was in residual tension while the composite was in residual compression. The secondary modulus was determined to be 5.25×10^6 psi which was well below the predicted value of 13.6×10^6 psi based upon linear strain-hardening of the aluminum alloy. This indicates that extensive fiber breakage occurred at the knee. The specimens failed at a strain of 4,000 μ in/in

which was far below the predicted value of 8,877 μ in/in including residual thermal strain. The ultimate stress obtained was 47.0 ksi. From the SQ5 laminate program the predicted failure stress is 146.9 ksi. While based on failure of the 0° plies with thermal stress and strain-hardening behavior of the aluminum, the predicted value is 135.2 ksi. The difference in the predictions is due to the fact that SQ5 is a linear analysis program. It is believed that extensive fiber breakage was the main factor leading to the early failure of these laminates.

Transverse strain was also presented in the figure as a function of stress. Poisson ratio was essentially constant during the test; the average value ν_{xy} for all tests was 0.27 compared to the predicted value of 0.31.

4.3.3 [90/Aℓ] Laminates

Figure 16 shows the predicted and a typical experimentally determined stress-strain diagram for the $[90_4/A\ell]_s$ laminate (V_c = 0.50). The experimentally determined modulus was 6.05 x 10^6 psi while the predicted value is 6.5 x 10^6 psi. The curve is linear up to a strain of 4,550 μ in/in which corresponds to failure of the 90° plies. The calculated residual thermal stress is tensile for the 90° plies. With thermal strain included the 90° plies are predicted to fail at a strain of 3,200 μ in/in. The corresponding predicted failure stress is 20.5 ksi for this laminate. The ultimate stress obtained was 28.0 ksi. From the SQ5 laminate analysis program, the predicted value is 26.5 ksi which is close to the experimental value even though

thermal stress is not included. These results indicate that the actual thermal strains are lower than the predicted values.

A transverse strain curve is also presented in the figure. It is linear. The experimentally determined Poisson ratio ν_{xy} is 0.085 which compares fairly well with the predicted value of 0.11.

4.3.4 $[45_2/-45_2/A\ell]_s$ Laminates

Figure 17 presents the theoretical and experimental stress-strain behavior of the $[45_2/-45_2/A\ell]_s$ (V_c = 0.50) laminate. The curve is essentially linear up to a strain of 5,000 μ in/in and then exhibits sharp nonlinearity to failure at an average ultimate strain of 16,000 μ in/in. The experimentally determined modulus of elasticity was 6.93 x 10^6 psi compared to the predicted value of 7.15 x 10^6psi. The residual thermal stresses were not significant (Table 4) due to the similarity in coefficients of thermal expansion. The average ultimate stress was 47.5 ksi which is slightly higher than the predicted value of 43.0 ksi based on the ultimate stress contributions from the $[45_2/-45_2]$ laminate and the aluminum alloy. The ultimate strains obtained were 15,200 μ in/in, 16,400 μ in/in and 19,200 μ in/in which were in the range of the ultimate strains obtained for the $[45_2/-45_2]_s$ laminates (Table 3). The failure stress obtained from SQ5 program does not agree with the experimental value because the SQ5 is a linear analysis program. Both the aluminum and the $[45_2/-45_2]_s$ laminate exhibit nonlinear behavior prior to failure.

The transverse strain ε_y is also presented in the figure as a function of stress. The stress-strain behavior is similar to that of the axial strain. The Poisson ratio ν_{xy} was essentially constant during the tests with a value of 0.56 which compares well with the predicted value of 0.52.

4.3.5 [0/90/Aℓ] Laminates

There were three configurations for this type of laminate: $[0_3/90/A\ell]_s$, $[0_2/90_2/A\ell]_s$ and $[90_2/0_2/A\ell]_s$ (V_c = .50). The purpose of these tests was two fold: first, to determine the influence of 90° plies between the unidirectional (0°) reinforcement and the metal; second, to determine the influence of stacking sequence. The predicted and experimentally determined curves for these laminates are compared in Figures 18 and 19.

As shown in Table 4, the results obtained were very consistent. For the $[0_3/90/A\ell]_s$ laminate, the average experimentally determined elastic modulus was 15.65 x 10^6psi which agreed well with the predicted value of 15.5 x 10^6psi. Both specimens tested exhibited initial linear stress-strain behavior which was followed by gradual nonlinearity to failure. The proportional limit occurred at strains of 2,150 μ in/in and 2,400 μ in/in. From residual thermal stress analysis, the 90° plies and the aluminum are in residual tension. (The thermal strains are shown in Table 4 for each different ply). Based on failure of the 90° plies at strains of 4,000 μ in/in, these plies should fail at an additional strain of 1,020 μ in/in. The proportional limit is expected to be due to failure of these 90° plies since the aluminum has not yielded at this strain. Thus the experimental results appear to indicate that the actual thermal stresses were lower than the predicted values. The average ultimate stress and strain were 50.0 ksi and 3,500 μ in/in, respectively. These values are far below the predicted values of 109.4 ksi and 9,120 μ in/in, based on failure of the

0° plies. The ultimate strain was also far below the ultimate strain obtained for the all composite $[0_3/90]_s$ laminate (Table 3 and Fig. 21). Based on failure of the 90° plies, the SQ5 program predicts an ultimate stress of 62.12 ksi without considering residual thermal stresses. This value is slightly higher than the experimental value. The failure is believed to be due to fiber breakage and/or debonding initiated by the failure of the 90° plies. Unlike the $[0_4/A\ell]_s$ laminates, these laminates with 90° plies did not exhibit a distinct knee prior to failure.

Transverse strain is also presented as a function of stress in Figure 18. The Poisson ratio ν_{xy} was essentially constant during the tests yielding a value of 0.204. The predicted value is 0.21.

For the $[0_2/90_2/A\ell]_s$ and the $[90_2/0_2/A\ell]_s$ laminates, Table 4 shows that all the results obtained were extremely consistent. The average elastic moduli were 12.4 x 10^6 psi and 12.5 x 10^6 psi for the $[0_2/90_2/A\ell]_s$ and the $[90_2/0_2/A\ell]_s$ laminates, respectively. The predicted value is 12.6 x 10^6 psi for both configurations. For the $[0_2/90_2/A\ell]_s$ laminates, nonlinearity occurred at a strain of 3,000 μ in/in for both specimens tested. This may correspond to failure of the 90° plies and/or nonlinearity of the aluminum. From residual thermal stress analysis, the 90° plies and the aluminum were in residual tension with residual tensile strains of 2,630 μ in/in and 1,550 μ in/in respectively (Table 4). Based on failure of the 90° plies at strains of 4,000 μ in/in, they can only carry an additional strain of approximately 1,370 μ in/in. The aluminum has not yielded at an applied strain of 3,000 μ in/in. Thus the first nonlinearity appears

to correspond to failure of the 90° plies and the results indicated that the actual thermal stress was lower than the predicted value. The average ultimate stress and strain were 47.0 ksi and 4,000 μ in/in. These values are far below the predicted values of 85.7 ksi and 9,800 μ in/in based on the failure of the 0° plies. However the ultimate strain is slightly greater than the average ultimate strain of the $[0_2/90_2]_s$ laminates which failed at 3,450 μ in/in (Fig. 22). From the SQ5 program with failure based upon the 90° plies, the predicted value is 50.4 ksi which agrees fairly well with the experimental value.

For the $[90_2/0_2/A\ell]_s$ laminates, the results obtained were also consistent. The stress-strain curves exhibited an initial linear portion followed by a gradual nonlinearity to failure. The proportional limit occurred at an average strain of 2,800 μ in/in. From residual thermal stress analysis, the aluminum has not yielded at this strain. Thus the proportional limit appears to correspond to failure of the 90° plies. Both specimens failed at an ultimate stress of 47.0 ksi and the ultimate strains obtained were 4,100 μ in/in and 4,400 μ in/in. These values were, in general, lower than the ultimate strains obtained for the $[90_2/0_2]_s$ laminates (Table 3 and Fig. 23). The SQ5 program predicts the same failure stress as for the $[0_2/90_2/A\ell]_s$ laminate. There were no significant differences in mechanical behavior between the $[0_2/90_2/A\ell]_s$ and the $[90_2/0_2/A\ell]_s$ laminates. It would appear taht the effects of the interlaminar normal stress σ_z were not as significant as they were for the $[0_2/90_2]_s$ and $[90_2/0_2]_s$ laminates (sect. 4.2.4). Another observation is that no distinct knee occurred

on the stress-strain curve as was observed in the $[0_4/A\ell]_s$ laminate (Fig. 22). It would appear that failure of these composite reinforced metal laminates is initiated by the failure of the 90° plies. There was good correlation between the experimental results for ultimate stress and the value predicted using the SQ5 program. The influence of fiber breakage and/or debonding may be explained by future acoustic emission investigations.

Transverse strain ε_y is also presented as a function of stresses in Figure 19. The Poisson ratio ν_{xy} was essentially constant during the tests. The average values for ν_{xy} was 0.14 for the $[0_2/90_2/A\ell]_s$ and the $[90_2/0_2/A\ell]_s$ laminates while the predicted value is 0.16 for both laminates.

4.3.6 $[45_2/-45_2/90/A\ell]_s$

Figure 20 presents the predicted and experimental stress-strain diagrams for the $[45_2/-45_2/90/A\ell]_s$ (V_c = .625) laminate. Two specimens were tested and the results obtained were consistent (Table 3). Both curves exhibited an initial linear portion followed by gradual nonlinearity to failure. The average experimentally determined modulus was 7.1 x 10^6 psi which agreed well with the predicted value of 7.2 x 10^6 psi. From residual thermal stress analysis, the ±45° plies were in residual compression; the 90° plies and the aluminum alloy were in residual tension. The proportional limit occurred at a strain of 2,800 μ in/in which is believed to correspond to failure of the 90° plies with thermal strain included. The ultimate stress obtained was 46.0 ksi which is slightly higher than the

predicted value of 42.5 ksi based on stress contributions from the $[45_2/-45_2/90]_s$ laminate and the aluminum alloy including strain-hardening effects. From the SQ5 program the predicted ultimate stress is 28.8 ksi which is based on failure of the 90° plies at the ultimate strain of 4,000 μ in/in. The laminates failed at strains of 7,800 μ in/in and 9,000 μ in/in which are far below the ultimate strain of the $[45_2/-45_2]_s$ laminate but well above the ultimate strain of the all composite $[45_2/-45_2/90]_s$ laminate (Table 3 and Fig. 24).

Transverse strain ε_y is also presented in figure 20. Poisson ratio ν_{xy} is essentially constant with a value of 0.42 which compared well with the predicted value of 0.40.

Figure 24 presents the comparison of results of all laminates consisting of ±45° plies. As can be seen from the figure, when 90° plies are added to the laminate, the ultimate strain is reduced. This early failure is believed to be due to fiber breakage initiated by rupture of the 90° plies and/or interlaminar stresses.

This figure also shows that the aluminum has a positive influence in that it increases both the stiffness and the strength of laminates with ±45° plies.

4.4 Failure Modes

Four modes of failure are observed during this investigation. The unidirectional [0] specimens exhibited both transverse fracture and longitudinal splitting along the fibers. Other specimens with 0° and 90° plies exhibited a failure surface which was normal to the direction of loading. All specimens with ±45° plies failed along the

45° lines. The $[45_2/-45_2]_s$ specimens failed along a single 45° line. Other specimens with ±45° plies generally failed along alternating ±45° lines.

Failure occurred in the test section and near the grips but there was no correlation between magnitude and location of the failure. While some specimens exhibited limited debonding after failure, it could not be ascertained if debonding occurred prior to or after failure.

5. SUMMARY AND CONCLUSIONS

The main results of the experimental investigation on composite reinforced metal laminates are summarized in Figures 21 to 24. These figures show that the composite reinforced aluminum laminates $[0_2/90_2/A\ell]_s$, $[45_2/-45/A\ell]_s$ and $[45_2/-45_2/90/A\ell]_s$ have greater strength than their all composite counterparts, but the composite reinforced aluminum laminates $[0_4/A\ell]_s$, $[0_3/90/A\ell]_s$ and $[90_2/0_2/A\ell]_s$ have lower strength than their all composite counterparts.

The greatest reduction in strength occurs for the $[0_4/A\ell]_s$ and $[0_3/90/A\ell]_s$ laminates. All composite reinforced aluminum laminates with 0° plies failed at ultimate strains of 4,400 μ in/in or lower (See Table 3). This is approximately fifty percent of the ultimate strain of the unidirectional (0°) boron/epoxy. These early failures are believed to be due to edge effects which initiate fiber breakage and/or local debonding. These edge effects are due to the thermal and mechanical mismatch in the transverse direction. When this mismatch is reduced, as for the laminates with ±45° plies and the $[90_4/A\ell]_s$ laminates, there is no degradation in strength. Analysis of the acoustic emissions which were recorded on tape during this investigation should shed more light on the question of fiber breakage and debonding.

The distinct knee which is exhibited in the behavior of $[0_4/A\ell]_s$ laminates indicates large scale fiber breakage at the knee. While other configuration did exhibit nonlinear behavior, the nonlinearities were much more gradual and could be attributed to other factors such

as failure of 90° plies and the inherent nonlinearity of ±45° plies and aluminum.

The distinct knee for the $[0_4/A\ell]_s$ laminates appears to indicate a mode of failure different from the other laminates with 0° plies. The laminates with 0° and 90° plies exhibit more gradual nonlinearity which would be indicative of progressive failure of 90° plies. This conclusion is supported by the fact that the laminates with more 90° plies exhibited more nonlinearity prior to failure.

As indicated in Table 3, the $[0_3/90/A\ell]_s$ laminates exhibited greater ultimate stress than any of the other composite reinforced metal laminates. However, it should be noted that, except for the $[90_4/A\ell]_s$ laminates, the ultimate stress of all composite reinforced metal laminates fell within a very narrow range. The maximum ultimate stress was 51.0 ksi and the minimum value was 45.0 ksi. In contrast to this, the ultimate strains ranged from a maximum value of 19,200 μ in/in to a minimum value of 3,500 μ in/in. It is interesting to note that the laminate of maximum ultimate stress is also the laminate of minimum ultimate strain.

The stacking sequence of all composite bidirectional (0°,90°) laminates was shown to have a significant influence on the strength of these laminates. As shown in Figures 13 and Table 3, the $[90_2/0_2]_s$ laminates are stronger than the $[0_2/90_2]_s$ laminates. This difference in strength is attributed to the difference in interlaminar normal stress σ_z at the free edge of these two laminates. The laminate with compressive interlaminar normal stress σ_z is stronger than the laminate

with tensile interlaminar stress σ_z. The tensile interlaminar normal stress leads to debonding and early failure. This effect of stacking sequence was not evident in the composite reinforced metals. As indicated in Table 3 and Figure 19 the $[0_2/90_2/A\ell]_s$ and $[90_2/0_2/A\ell]_s$ laminates exhibited almost indentical ultimate stress value.

The results presented in Table 5 show that there was very good correlation between experimental and theoretical values for modulus and Poisson ratio for all laminates.

As expected, the experimental results of this investigation have shown that the maximum strain theory of failure as employed by the point stress laminate analysis program SQ5 is not reliable in predicting the ultimate stress of boron/epoxy reinforced aluminum. The experimental results have also shown that actual residual thermal stresses are lower than the predicted values.

Future work which should provide more insight into the strength of these composite reinforced metal laminates includes: experimental determination of transverse residual thermal strain; analysis of the interlaminar stresses at the free edge and comparison with known limiting values; analysis of the acoustic emission data obtained during this investigation; a study to determine the effect of panel width on the residual thermal stresses.

Material	Modulus of Elasticity (psi x 10^{-6})		Coefficient of Expansion (in/in/°F x 10^{6})	
	E_ℓ	E_t	α_ℓ	α_t
7075-T6 Aℓ	10.0	10.0	13.1	13.1
B/E* (0°)	26.7	2.53	2.5	17.0
B/E* (90°)	2.53	26.7	17.0	2.5
B/E* (±45°)	3.2	3.2	9.5	9.5

*NARMCO 5505/4

Table 1 Lamina Material Properties

Panel No.	Plies of B/E	Thickness of Aℓ (in)	Configuration
1	8		$[0_8]$
2	8		$[90_8]$
3	8		$[45_2/-45_2]_s$
4	8		$[0_3/90_1]_s$
5	8		$[0_2/90_2]_s$
6	8		$[90_2/0_2]_s$
7	10		$[45_2/-45_2/90]_s$
	Plies of B/E	Thickness of Aℓ (in)	
8	8	0.040	$[0_4/A\ell]_s$
9	8	0.040	$[90_4/A\ell]_s$
10	8	0.040	$[45_2/-45/A\ell]_s$
11	8	0.040	$[0_3/90_1/A\ell]_s$
12	8	0.040	$[0_2/90_2/A\ell]_s$
13	8	0.040	$[90_2/0_2/A\ell]_s$
14	10	0.04	$[45_2/-45_2/90/A\ell]_s$

Table 2 Test Specimen Configurations

Specimen No.	Configuration	Total Thickness (in)	E (10^6 psi)	σ_u (ksi)	ε_u μ in/in	ν_{xy}
101-1	$[0_8]$	.042	26.5	212	7900	.24
101-2		.042	26.5	222	8700	.21
101-3		.042	27.0	206	7600	.22
102-1	$[90_8]$	.042	2.5	7.6	3300	.02
102-3		.042	2.5	7.5	3150	.02
103-1	$[45_2/-45_2]_s$	.042	3.3	18.1	----	.83
103-2		.042	2.9	17.0	16100	.84
103-3		.042	3.4	17.3	16000	.86
104-1	$[0_3/90]_s$	.043	19.5	146	7800	.053
104-2		.045	20.0	108	6400	.075
104-3		.043	21.0	126	6800	.075
105-1	$[0_2/90_2]_s$	.046	15.0	38	3500	.04
105-2		.046	16.0	35	3400	.04
106-1	$[90_2/0_2]_s$	.045	13.0	70	6300	.036
106-2		.045	13.5	42	4400	.035
106-3		.045	14.0	58	6000	.034
107-1	$[45_2/-45_2/90]_s$	.054	4.8	19	4700	.46
107-2		.054	4.5	19	5000	.45

Table 3. Experimental Results of All Specimens Tested

Specimen No.	Configuration	Total Thickness (in)	E (10^6 psi)	σ_u (ksi)	ε_u (μ in/in)	ν_{xy}
108-1	$[0_4/A\ell]_s$	.084	18.5	49.0	4200	.270
108-2		.086	19.0	47.0	4000	.270
109-1	$[90_4/A\ell]_s$	.084	6.1	27.0	4400	.085
109-2		.086	6.0	28.5	4700	.085
110-1	$[45_2/-45_2/A\ell]_s$	.084	6.8	47.5	15200	.580
110-2		.084	6.8	47.8	19200	.530
110-3		.084	7.2	48.0	16400	.560
111-1	$[0_3/90/A\ell]_s$	.086	15.8	51.0	3500	.205
111-2		.085	15.5	50.0	3500	.203
112-1	$[0_2/90_2/A\ell]_s$	.085	12.3	47.0	4000	.139
112-2		.085	12.5	46.0	4000	.139
113-1	$[90_2/0_2/A\ell]_s$	.086	12.0	47.0	4100	.136
113-2		.086	13.0	46.0	4400	.136
114-1	$[45_2/-45_2/90/A\ell]_s$	.094	7.0	45.0	7800	.430
114-2		.094	7.2	47.0	9000	.420

Table 3. (Contin.) Experimental Results of all Specimens Tested

Specimen No.	Composite Volume Fraction V_c	Ultimate Stress (σ_u)(ksi)	Ultimate Strain (ε_u)(μin/in)	Residual Thermal Stresses (ksi)	Residual Thermal Strains (μin/in)	Total Stress (ksi)	Total Strain (μin/in)
101	1.0	213.0	8,070	-----	------	213.0	8,070
102	1.0	7.55	3,225	-----	------	7.55	3,225
103	1.0	17.2	16,000	-----	------	17.2	16,000
104	$\frac{0.75(0°)}{0.25(90°)}$	127.0	7,000	$\frac{-3.26}{9.30}$	$\frac{-123}{3,680}$	$\frac{171.5}{9.0}$	$\frac{6,877}{10,280}$
105	$\frac{0.50(0°)}{0.50(90°)}$	36.5	3,450	$\frac{-9.2}{8.9}$	$\frac{-347}{3,560}$	$\frac{82.0}{9.0}$	$\frac{3,103}{7,010}$
106	$\frac{0.50(0°)}{0.50(90°)}$	57.0	5,600	$\frac{-9.2}{8.9}$	$\frac{-347}{3,560}$	$\frac{139.0}{9.0}$	$\frac{5,253}{9,160}$
107	$\frac{0.80(\pm 45°)}{0.20(90)}$	19.0	4,850	$\frac{-1.07}{4.26}$	$\frac{-306}{1,700}$	$\frac{10.0}{9.0}$	$\frac{4,494}{6,500}$

Table 4. Average Experimental Results

Specimen No.	Composite Volume Fraction V_c	σ_u (ksi)	ε_u (μ in/in)	Residual Thermal Stresses (ksi)		Residual Thermal Strains (μ in/in)		Total Stress (ksi)		Total Strain (μ in/in)	
				Composite	Aℓ	Composites	Aℓ	Composite	Aℓ	Composite	Aℓ
108	0.50	47.0	4,000	-21.4	21.4	-807	2,140	87.3	58.0	3,193	6,140
109	0.50	28.0	4,550	2.17	-2.17	876	-217	9.0	43.3	5,426	4,333
110	0.50	47.5	16,000	-2.42	2.4	-690	240	17.2	65.0	15,310	16,240
111	0.375(0°) 0.125(90°)	50.0	3,500	0°:-27.8 90°:7.5	19.0	-1050 2,980	1,900	65.0 9.0	54.0	2,450 6,480	5,400
112	0.25(0°) 0.25(90°)	47.0	4,000	-37.0 6.6	15.5	-1,390 2,630	1,550	69.2 9.0	55.0	2,610 6,630	5,550
113	0.25(0°) 0.25(90°)	47.0	4,250	-37.0 6.58	15.5	-1.390 2,630	1,550	76.0 9.0	57.0	2,860 6,880	5,800
114	0.44(±45) 0.11(90°)	46.0	8,400	-2.61 3.17	1.84	-745 1,270	184	13.0 9.0	65.0	7,655 9,670	8,584

Table 4. (Continued) Average Experimental Results

Specimen No.	Configuration	$E_x \times 10^{-6}$ psi			ν_{xy}	
		Laminate Theory	Experimental Value	Rule of Mixture	Laminate Theory	Experimental Value
101	$[0_8]$	26.7	26.7	26.7	0.22	0.22
102	$[90_8]$	2.53	2.53	2.53	0.02	0.02
103	$[45_2/-45_2]_s$	3.3	3.2	----	0.78	0.85
104	$[0_3/90]_s$	20.7	20.2	20.5	0.062	0.067
105	$[0_2/90_2]_s$	14.6	15.5	14.5	0.036	0.04
106	$[90_2/0_2]_s$	14.6	13.5	14.5	0.036	0.035
107	$[45_2/-45_2/90]_s$	4.9	4.65	----	0.45	0.45
108	$[0_4/A\ell]_s$	18.4	18.75	18.25	0.31	0.27
109	$[90_4/A\ell]_s$	6.65	6.05	6.25	0.11	0.09
110	$[45_2/-45_2/A\ell]_s$	7.15	6.93	6.75	0.52	0.56
111	$[0_3/90/A\ell]_s$	15.5	15.65	15.26	0.21	0.20
112	$[0_2/90_2/A\ell]_s$	12.6	12.4	12.25	0.16	0.14
113	$[90_2/0_2/A\ell]_s$	12.6	13.0	12.25	0.16	0.14
114	$[45_2/-45_2/90/A\ell]_s$	7.2	7.1	----	0.40	0.42

Table 5. Comparison of Predicted Moduli and Poisson Ratios with Average Experimental Values

Specimen No.	Configuration	Experimental		Theoretical		
		σ_f (ksi)	ε_f (μ in/in)	σ_f (Eqn. 30 or 33) (ksi)	ε_f (Eqn. 32) (μ in/in)	σ_f (SQ5) (ksi)
101	$[0_8]$	213.0	8,070	------	------	-------
102	$[90_8]$	7.55	3,225	------	------	-------
103	$[45_2/-45_2]_s$	17.2	16,000	------	------	70.7
104	$[0_3/90]_s$	127.0	7,000	163.0	8,193	82.8
105	$[0_2/90_2]_s$	36.5	3,450	112.0	8,417	58.6
106	$[90_2/90_2]_s$	57.0	5,600	112.0	8,417	58.6
107	$[45_2/-45_2/90]_s$	19.0	4,850	13.0	16,306	19.6
108	$[0_4/A\ell]_s$	47.0	4,000	135.2	8,877	146.9
109	$[90_4/A\ell]_s$	28.0	4,550	20.5	3,200	26.5
110	$[45_2/-45_2/A\ell]_s$	47.5	16,000	43.0	16,690	120.0
111	$[0_3/90/A\ell]_s$	50.0	3,500	109.4	9,120	62.12
112	$[0_2/90_2/A\ell]_s$	47.0	4,000	85.7	9,800	50.4
113	$[90_2/0_2/A\ell]_s$	47.0	4,250	85.7	9,800	50.4
114	$[45_2/-45_2/90/A\ell]_s$	46.0	8,400	42.5	16,000	28.8

Table 6. Comparison of Ultimate Strength data for all Laminates

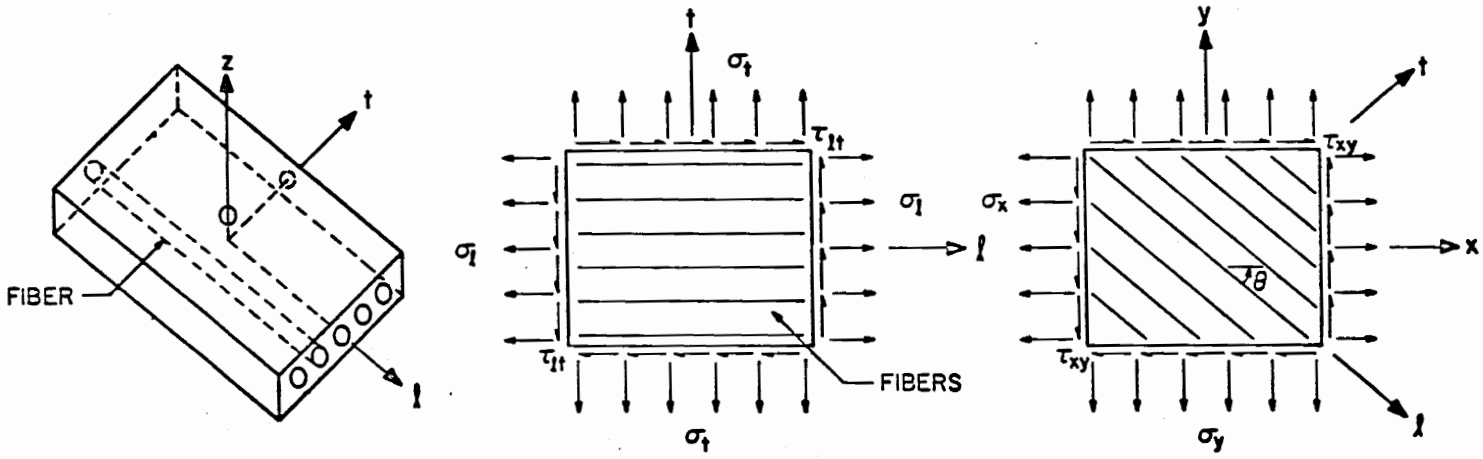

(a) ORTHOGONAL LAMINA

(b) NATURAL LAMINA COORDINATE SYSTEM

(c) TRANSFORMED LAMINA COORDINATE SYSTEM

FIG. 1 LAMINA COORDINATE SYSTEMS

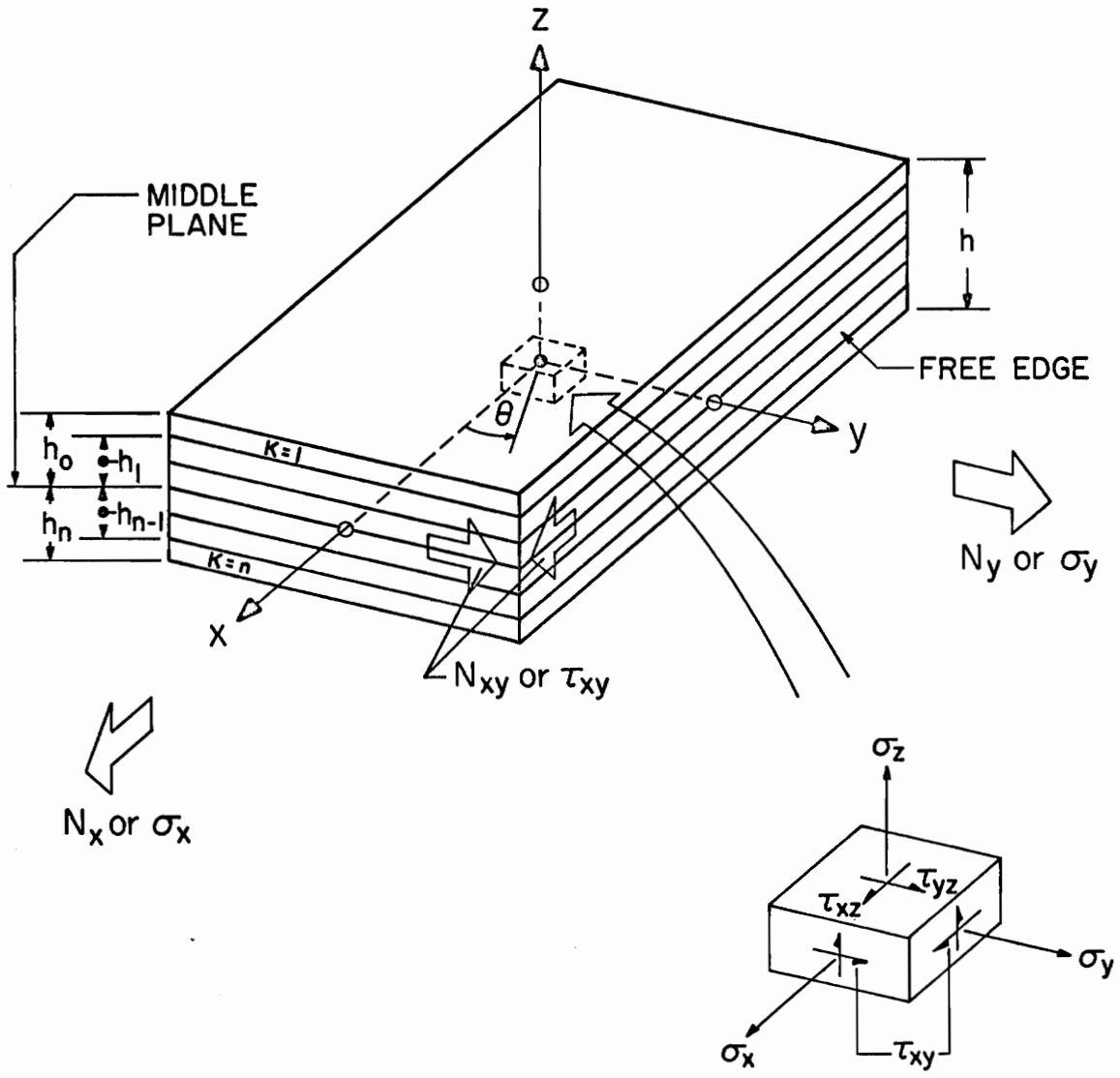

FIG. 2 LAMINATE GEOMETRY

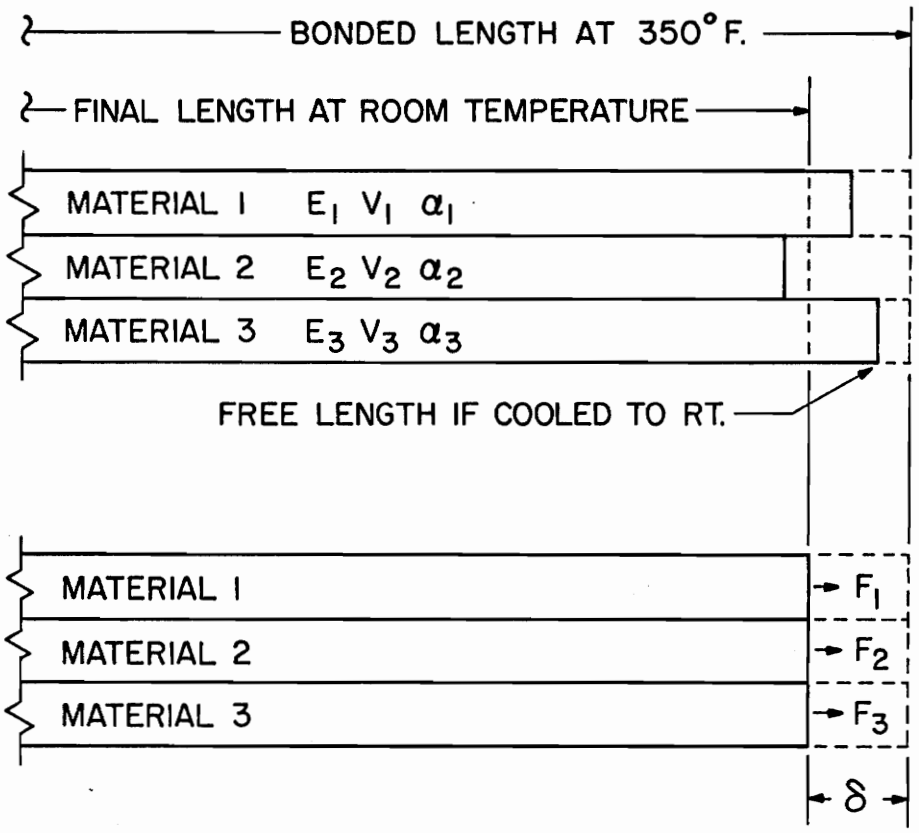

FIG. 3 THERMAL CONTRACTION OF INDIVIDUAL PLIES

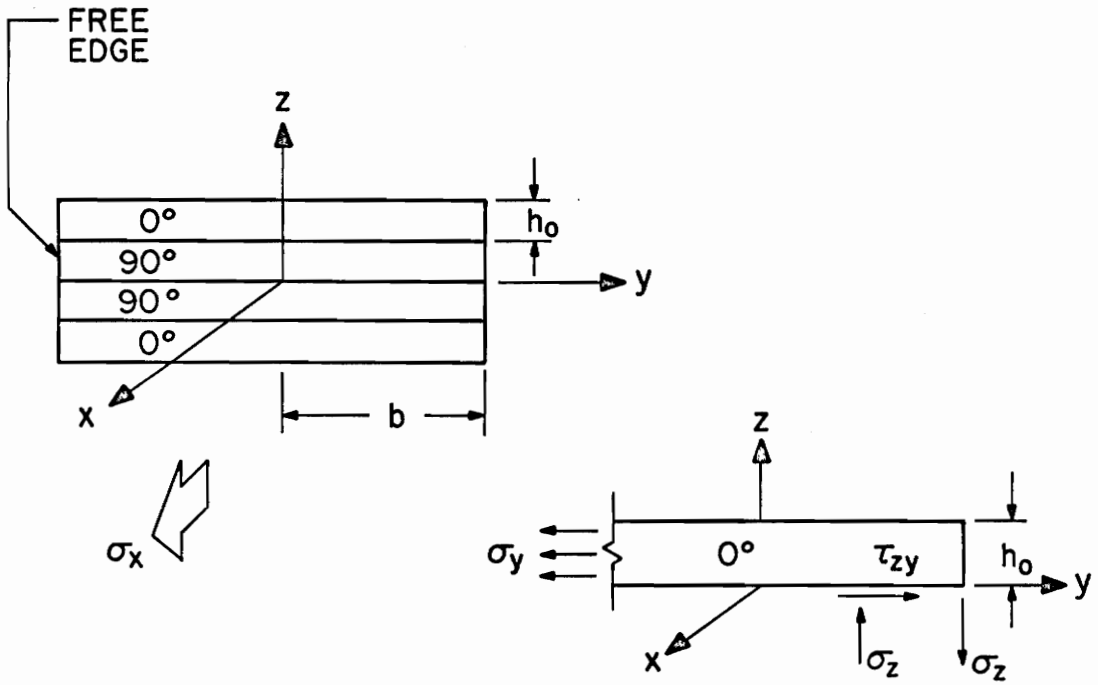

$\Sigma F_y = 0$

$\Sigma M_x = 0$

FIG.4 INTERLAMINAR NORMAL STRESS σ_z

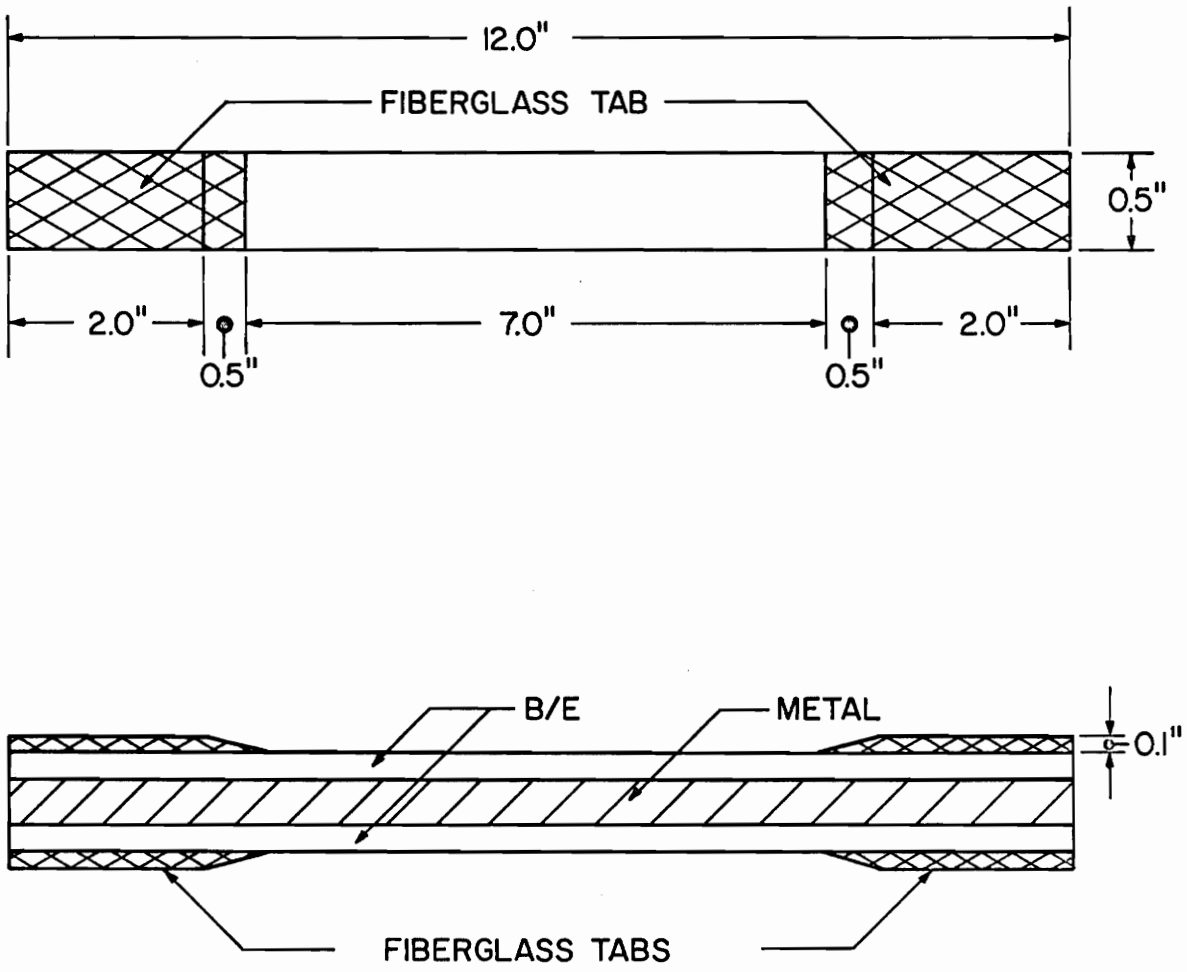

FIG. 5 TYPICAL DIMENSIONS OF COUPON SPECIMEN

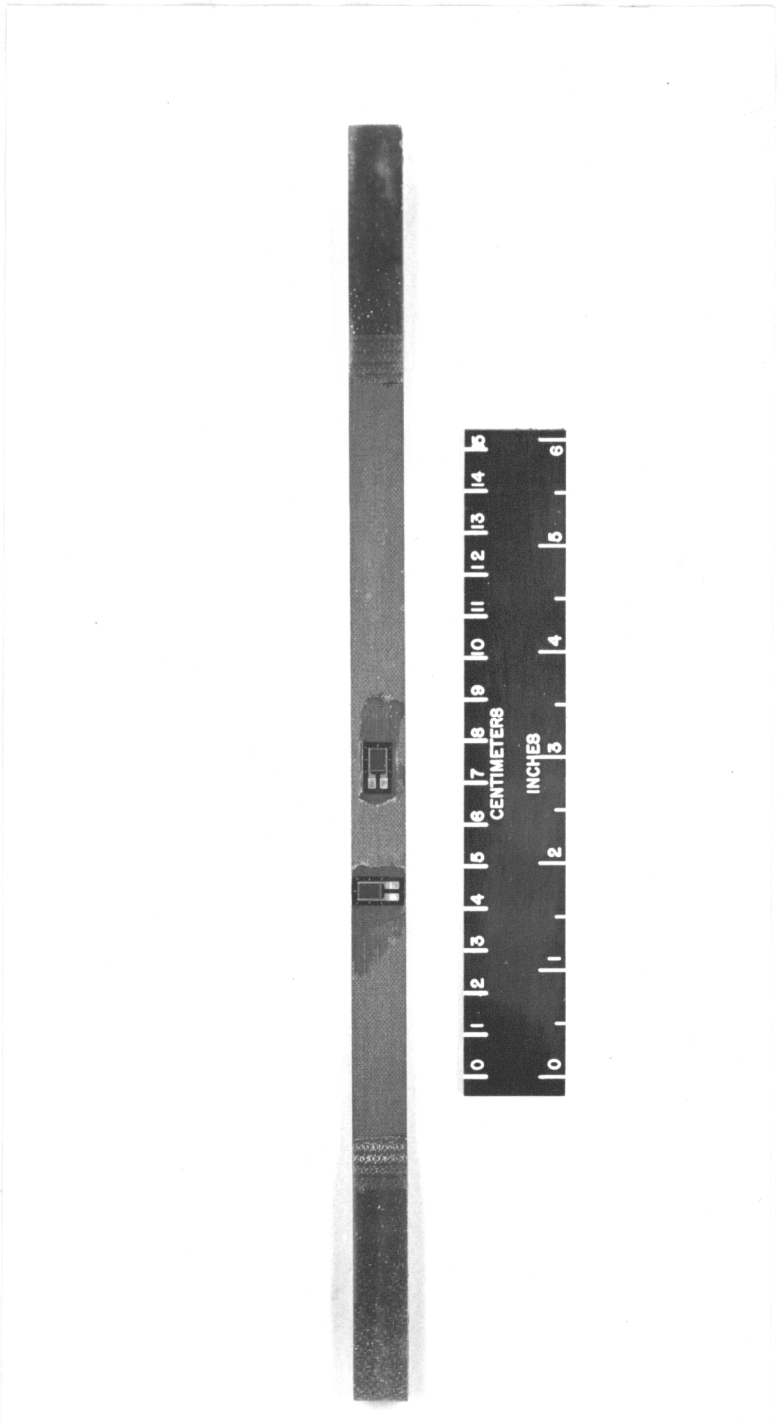

Figure 6. Typical Coupon Specimen

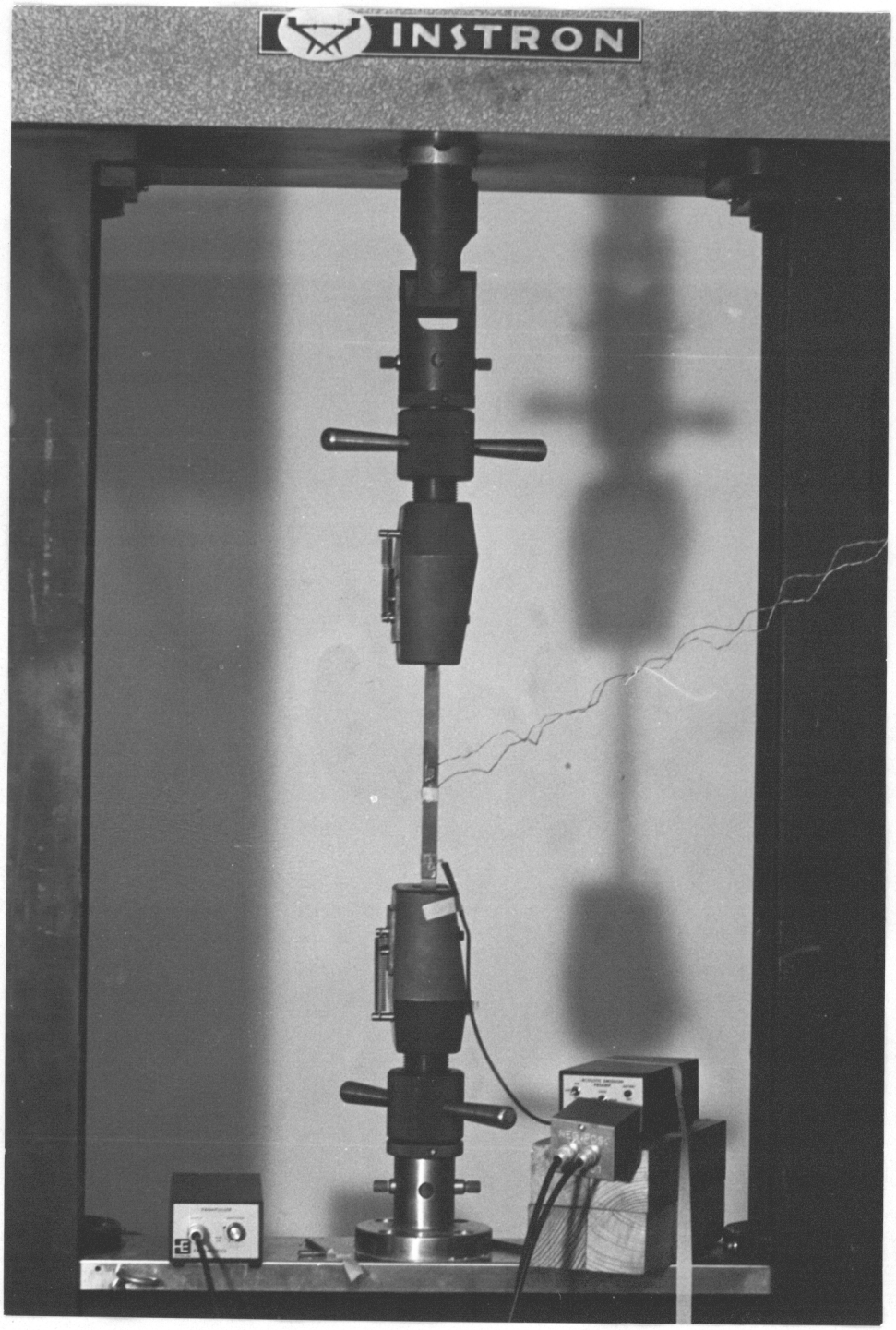

Figure 7. Test Setup

Figure 8. Equipments Used in Test Program

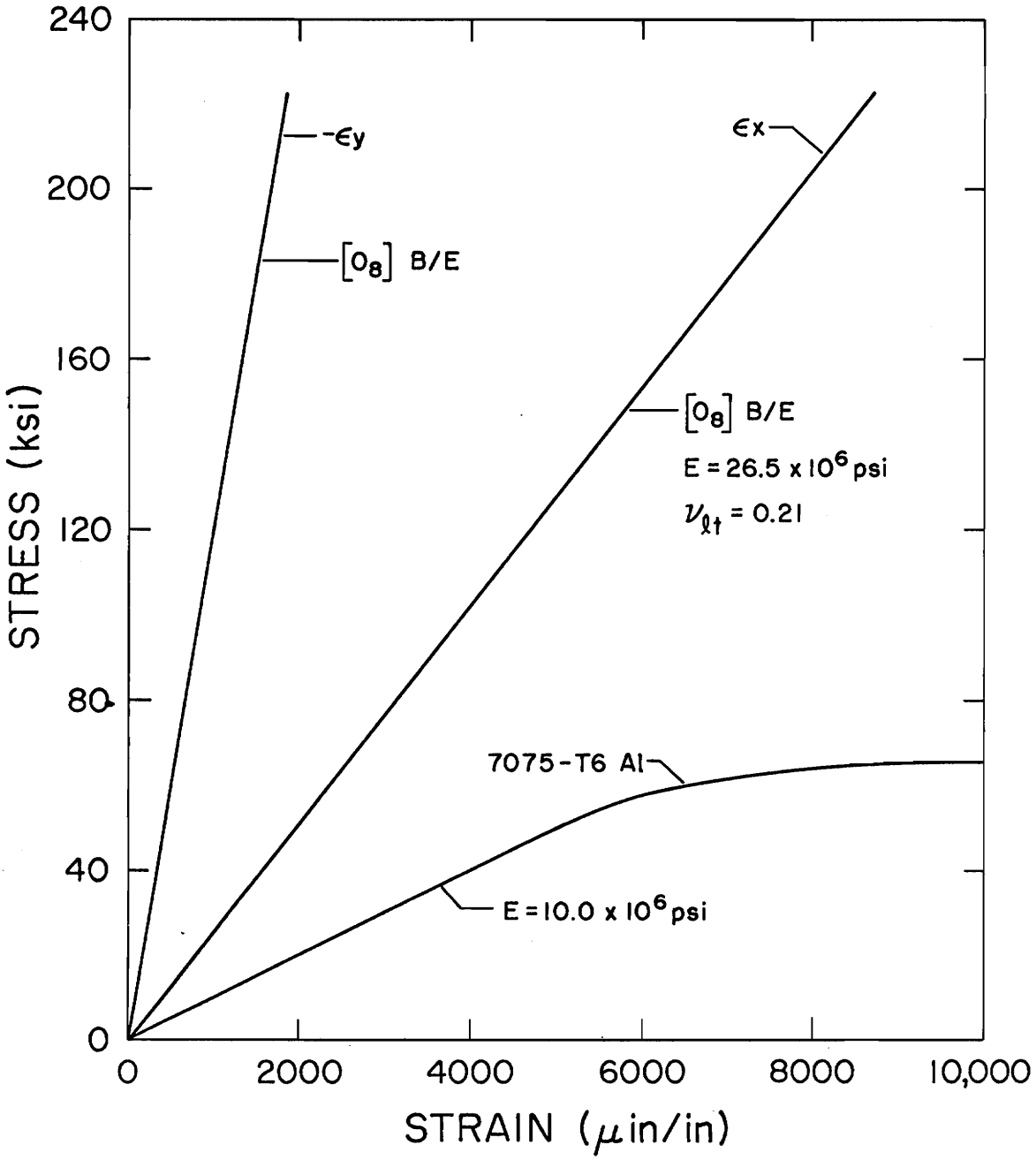

Figure 9. Stress-Strain Diagrams for Unidirectional [0] Boron/ Epoxy and 7075-T6 Aluminum

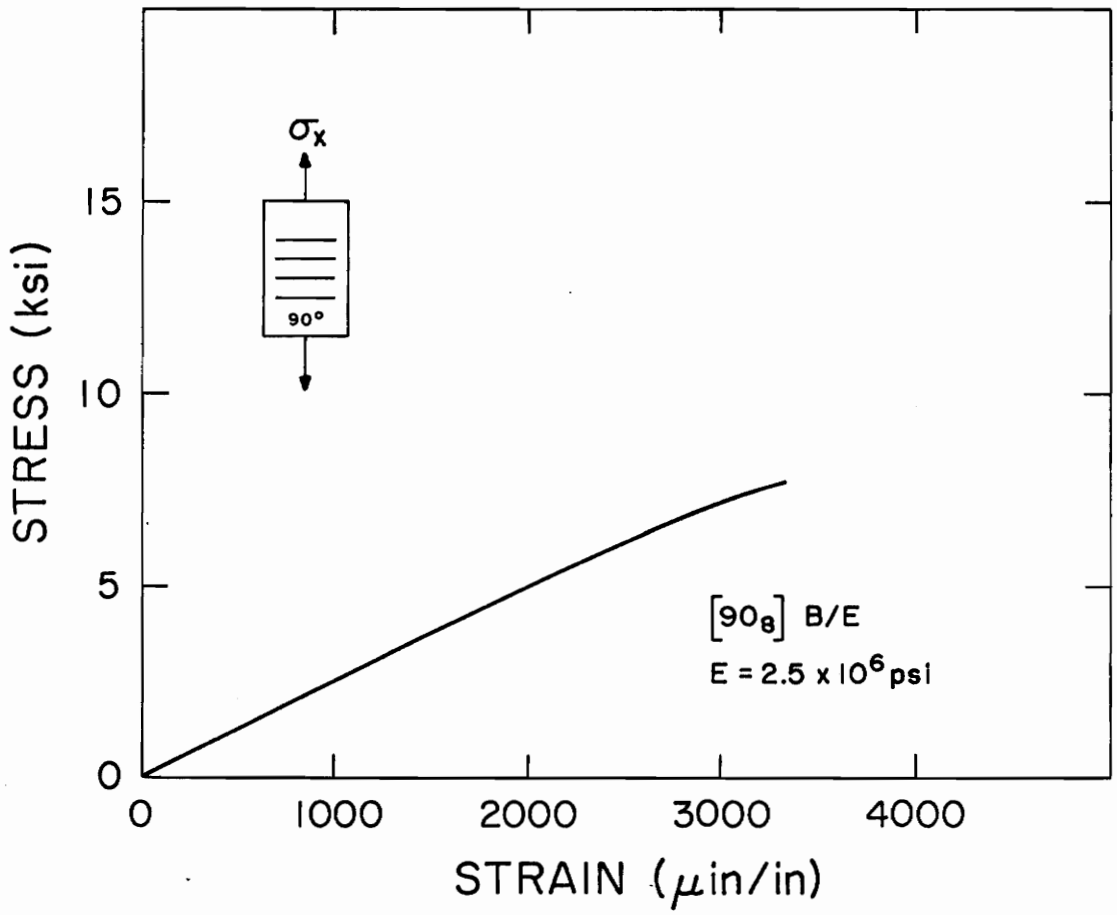

Figure 10. Stress-Strain Diagram for a [90] Boron/Epoxy Laminate

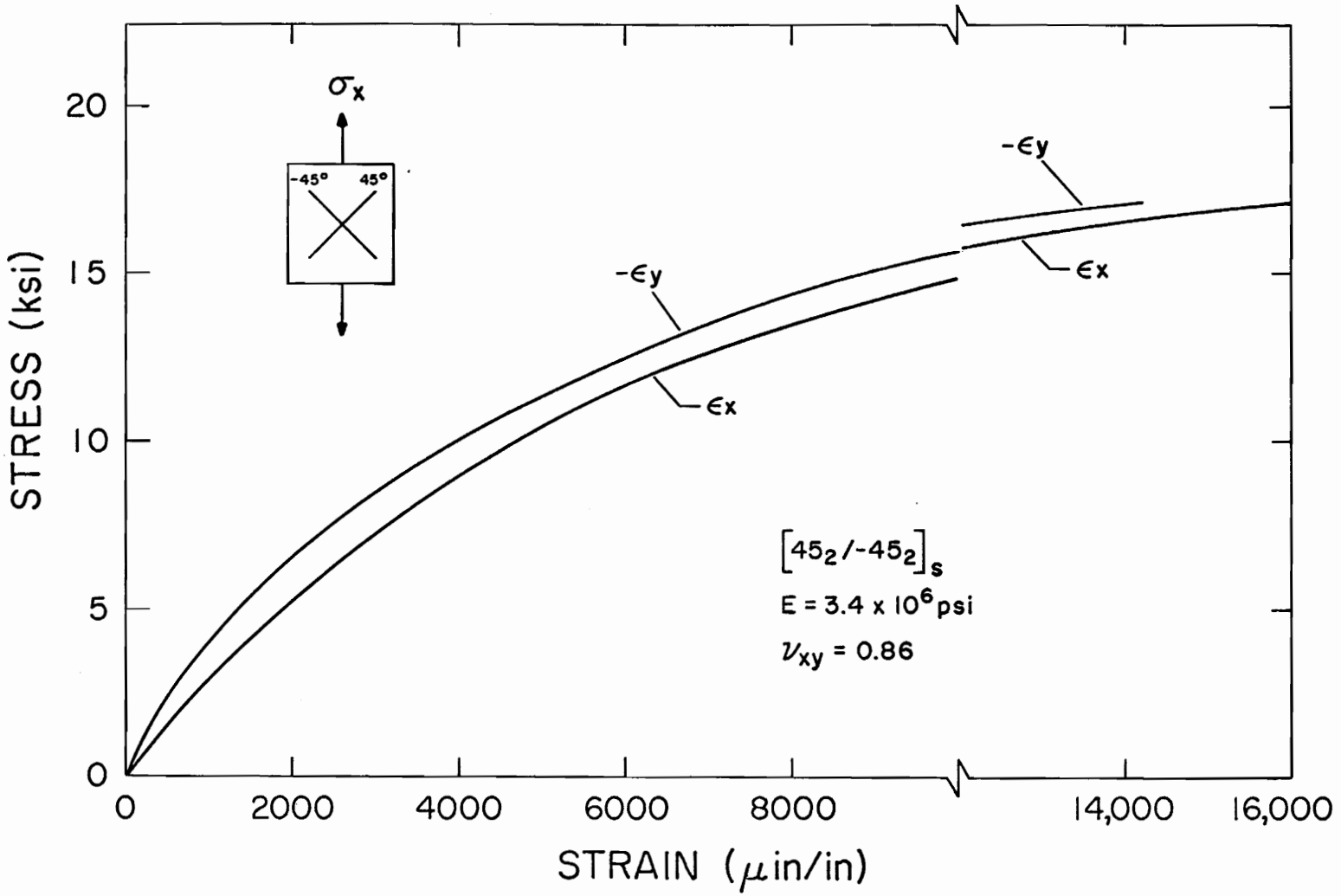

Figure 11. Stress-Strain Diagram for a $[45_2/-45_2]_s$ Boron/Epoxy Laminate

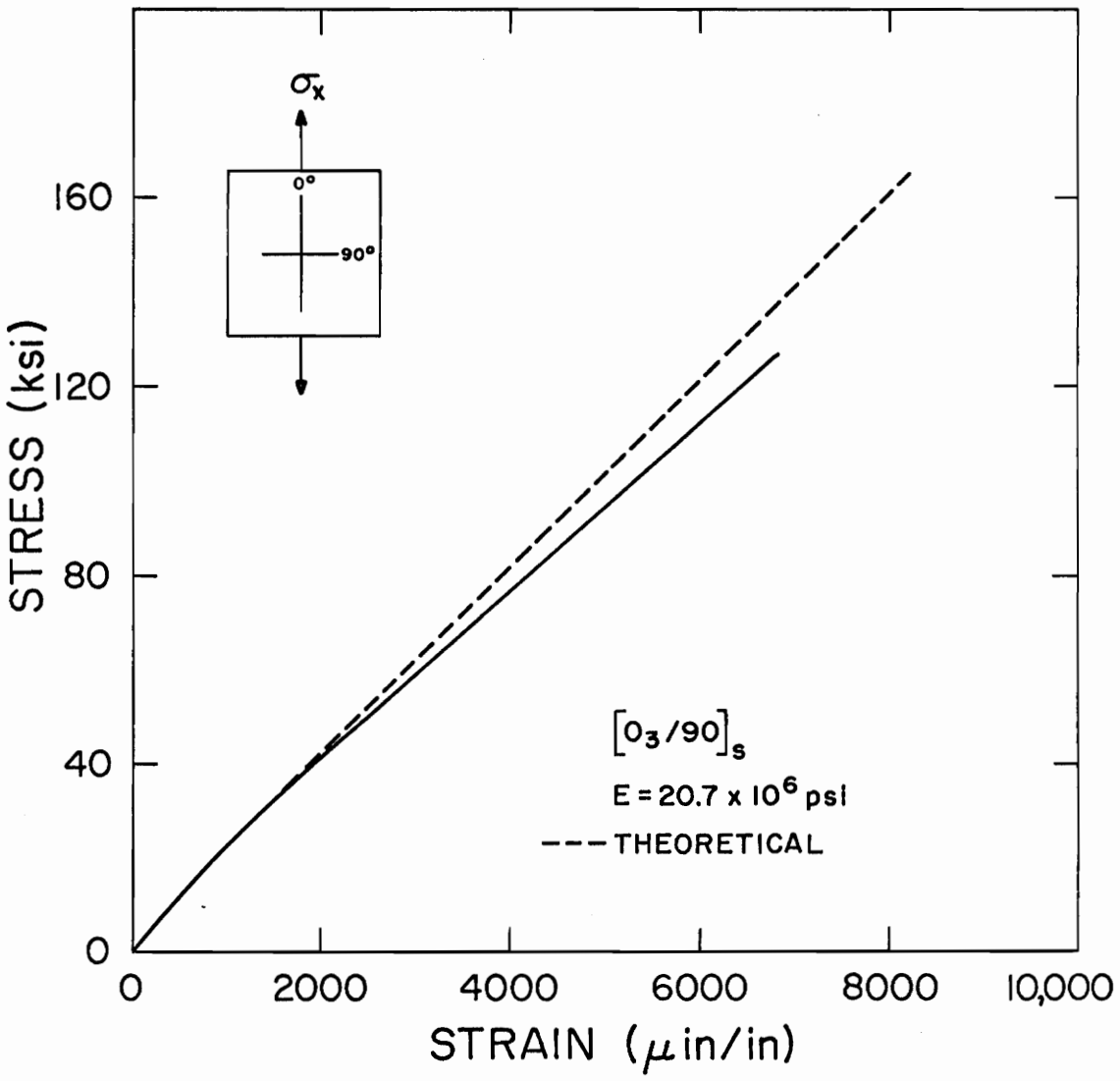

Figure 12. Stress-Strain Diagram for a $[0_3/90]_s$ Boron/Epoxy Laminate

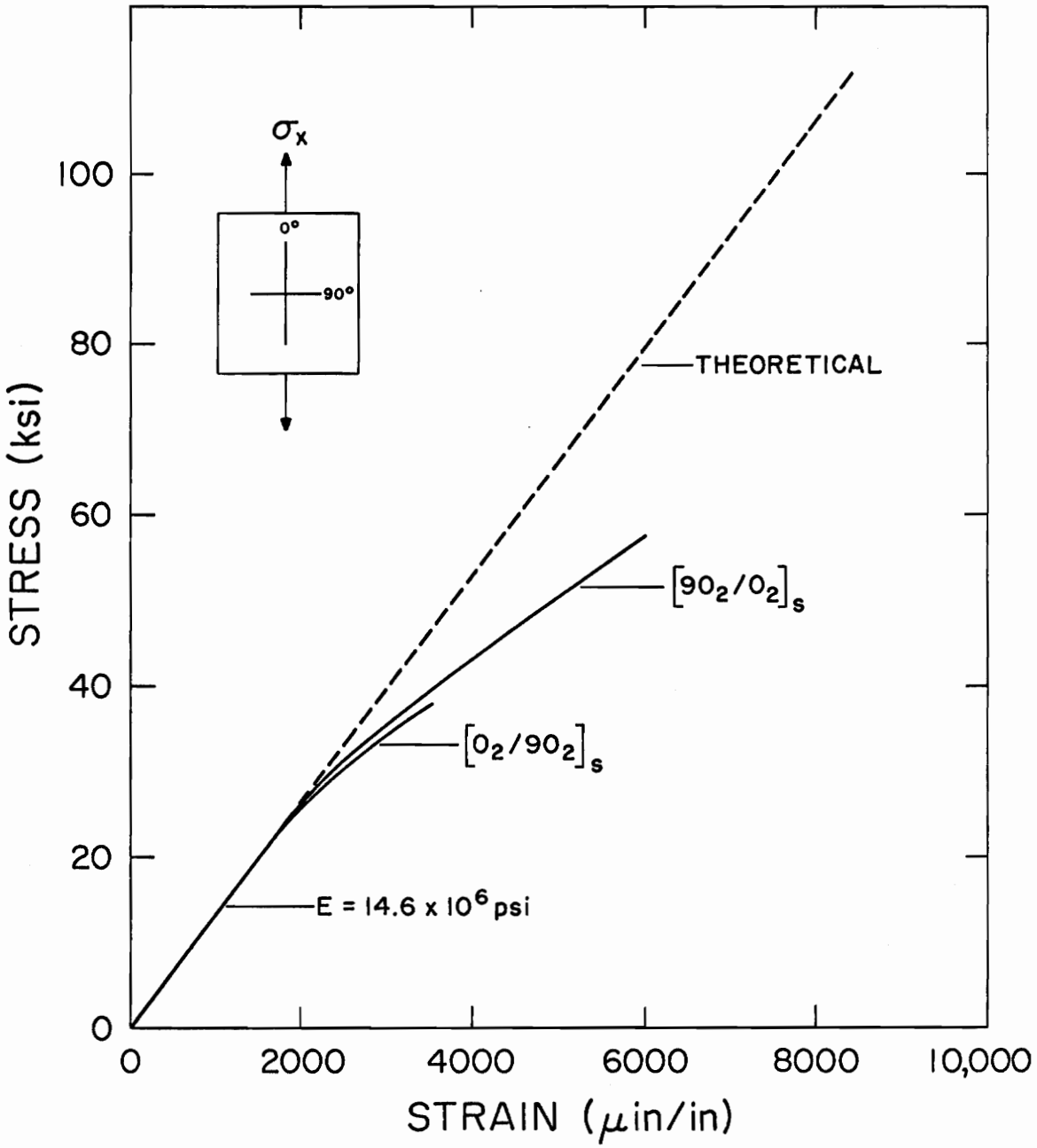

Figure 13. Stress-Strain Diagram for $[0/90]_s$ and $[90/0]_s$ Boron/Epoxy Laminates

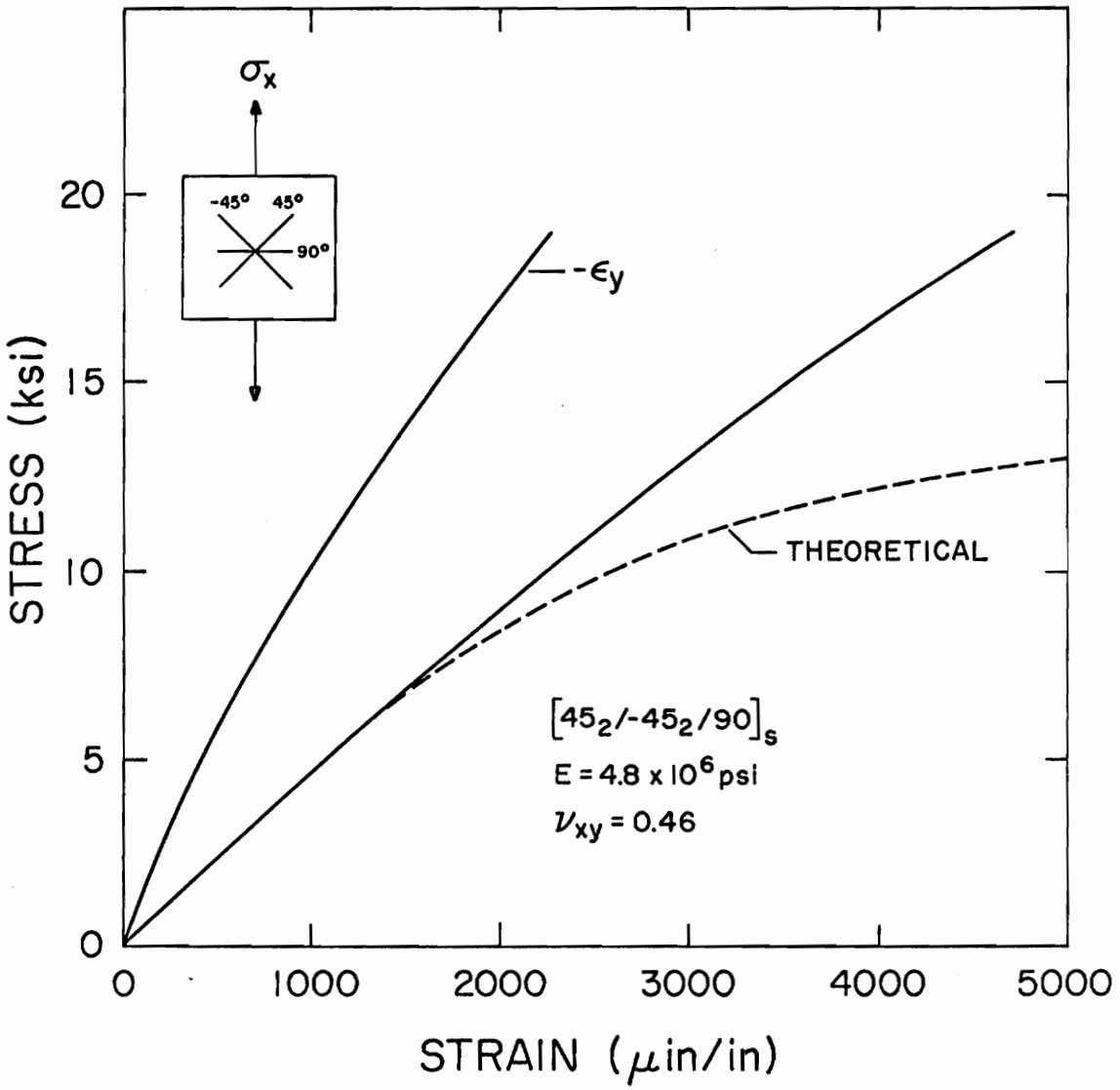

Figure 14. Stress-Strain Diagram for a $[45_2/-45_2/90]_s$ Boron/ Epoxy Laminate

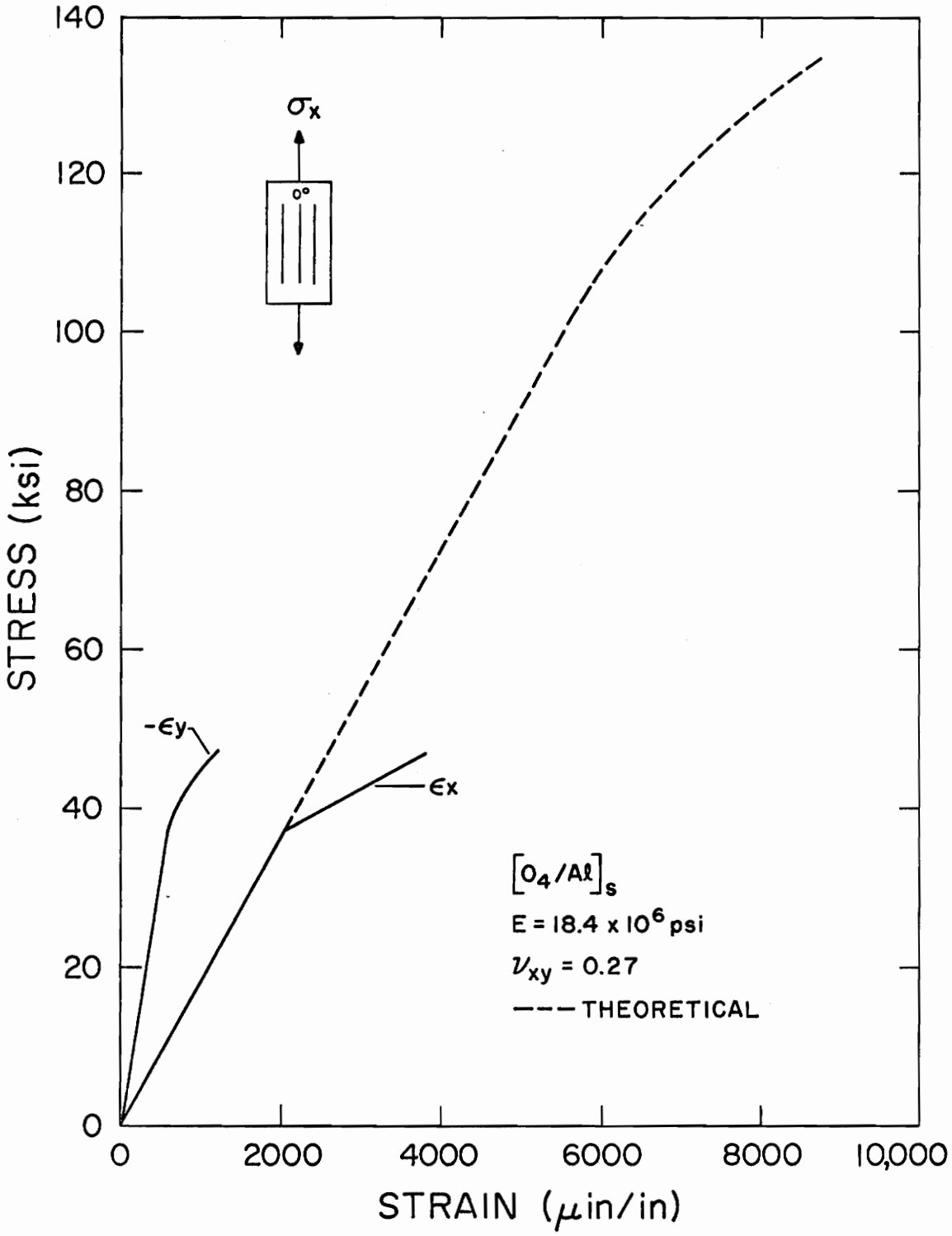

Figure 15. Stress-Strain Diagram for a $[0_4/A\ell]_s$ Boron/Epoxy reinforced Aluminum Laminate

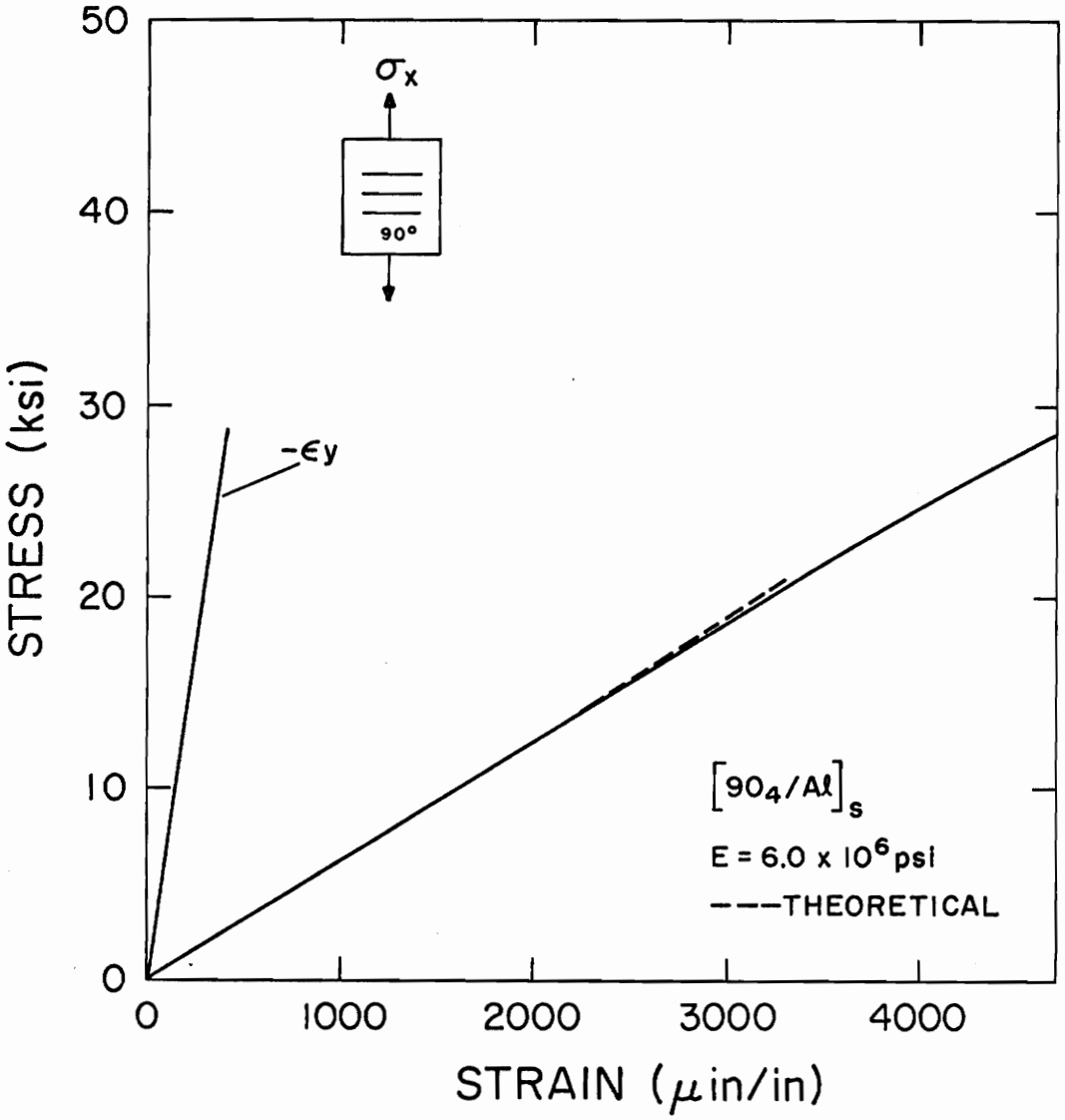

Figure 16. Stress-Strain Diagram for a $[90_4/A\ell]_s$ Boron/ Epoxy Reinforced Aluminum Laminate

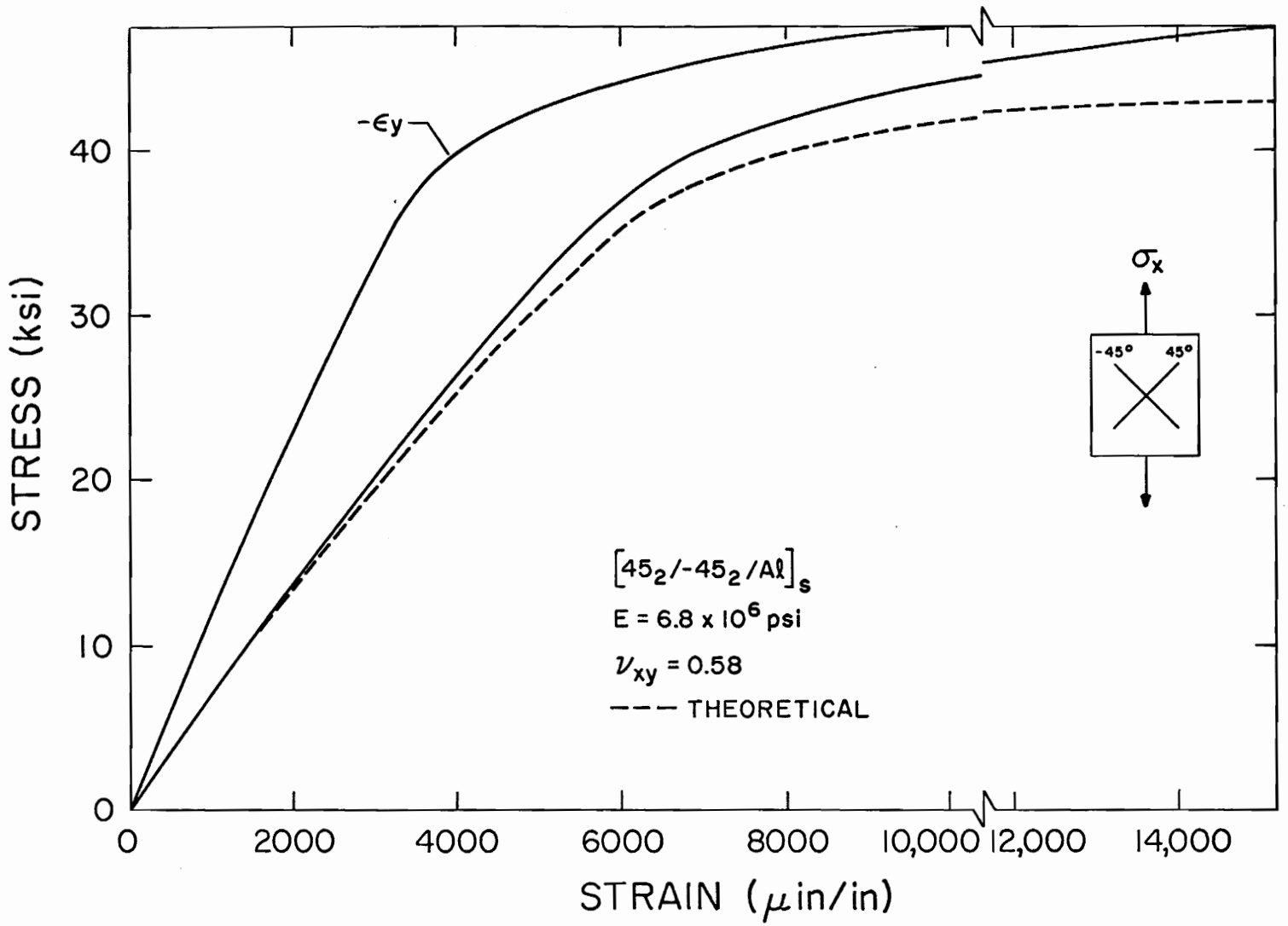

Figure 17. Stress-Strain Diagram for a $[45_2/-45_2/A\ell]_s$ Boron/Epoxy Reinforced Aluminum Laminate

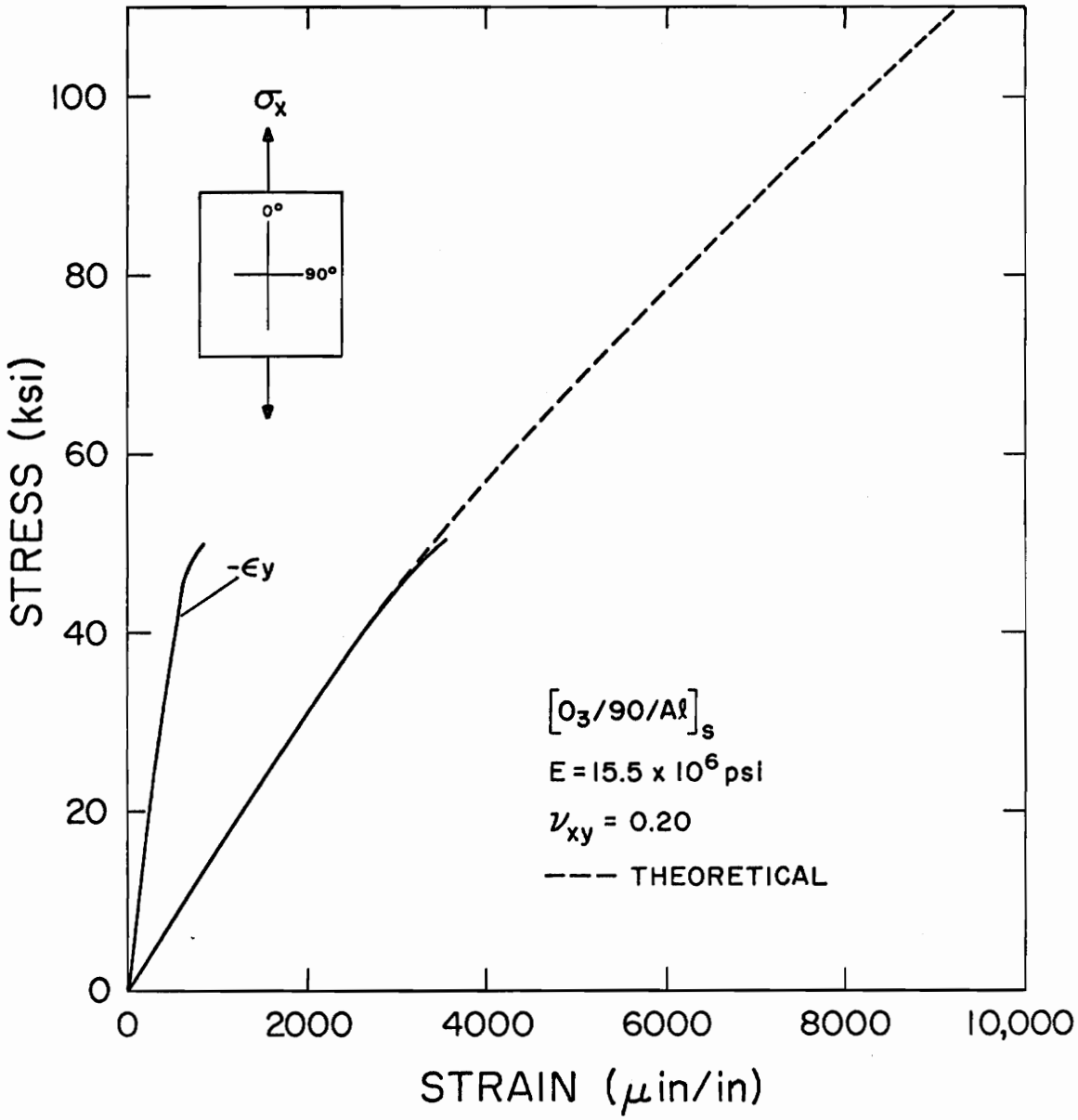

Figure 18. Stress-Strain Diagram for a $[0_3/90/A\ell]_s$ Boron/ Epoxy Reinforced Aluminum Laminate

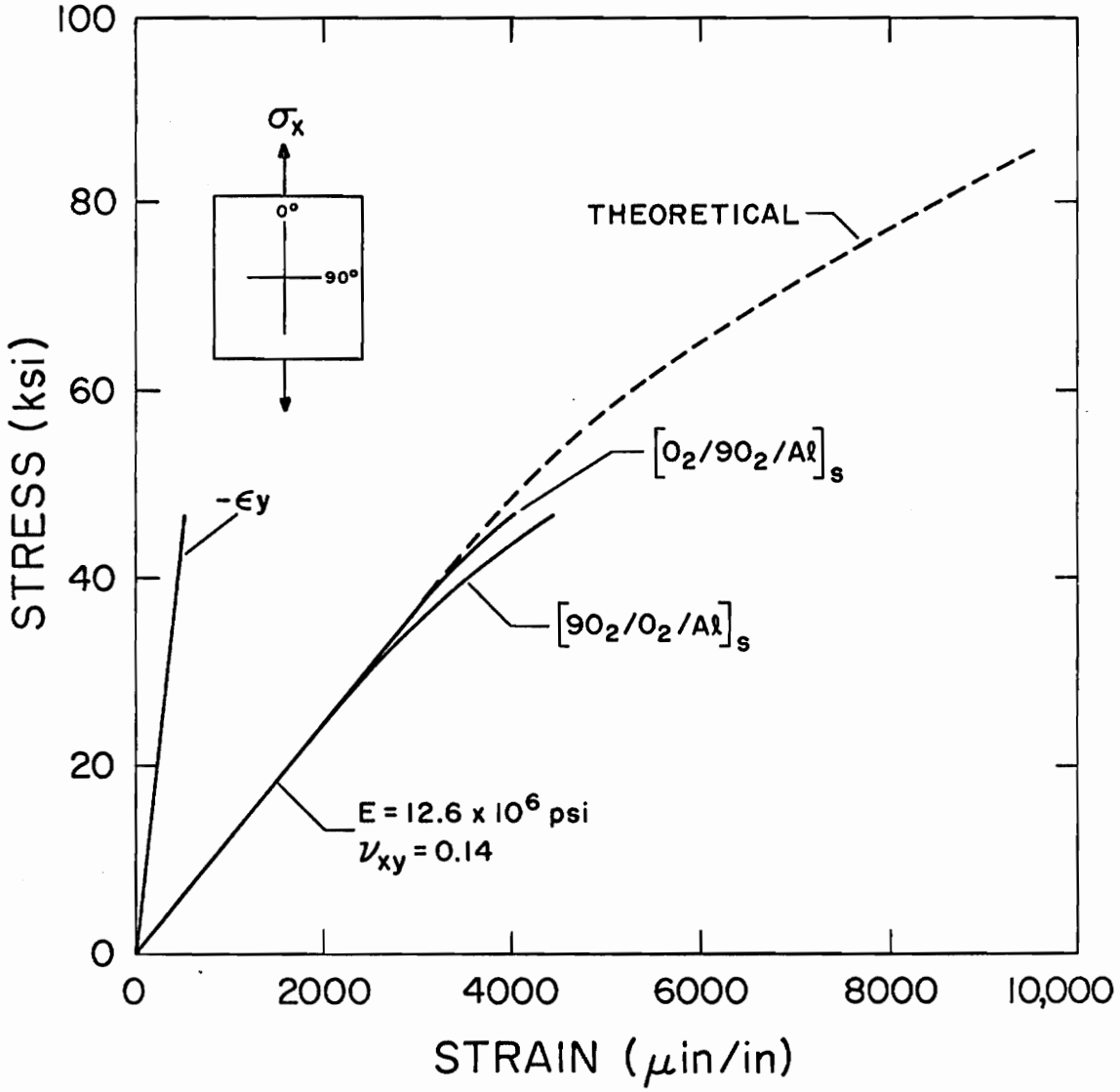

Figure 19. Stress-Strain Diagrams for $[0_2/90_2/A\ell]_s$ and $[90_2/0_2/A\ell]_s$ Boron/Epoxy Reinforced Aluminum Laminates

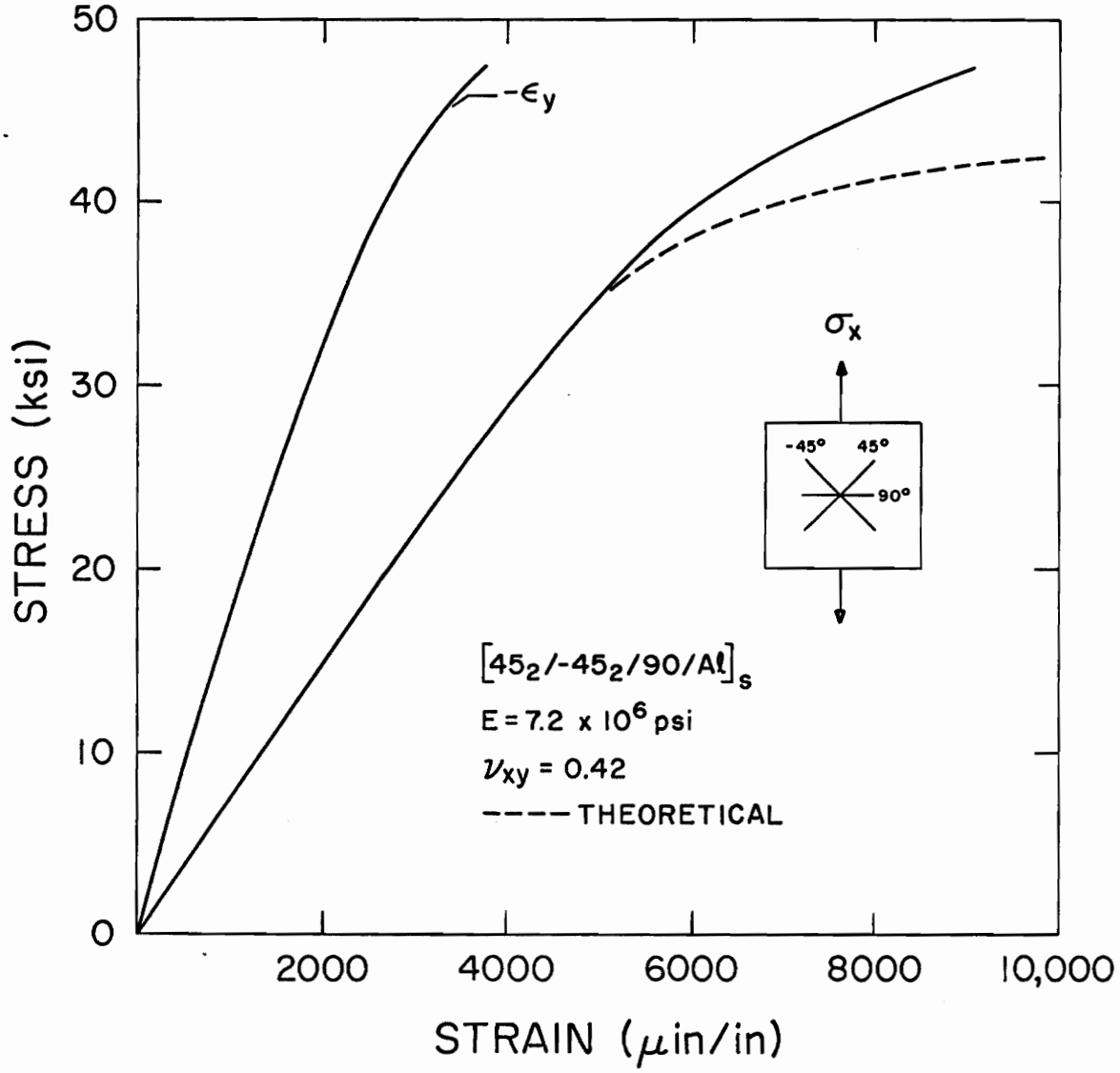

Figure 20. Stress-Strain Diagram for a $[45_2/-45_2/90/A\ell]_s$ Boron/Epoxy Reinforced Aluminum Laminate

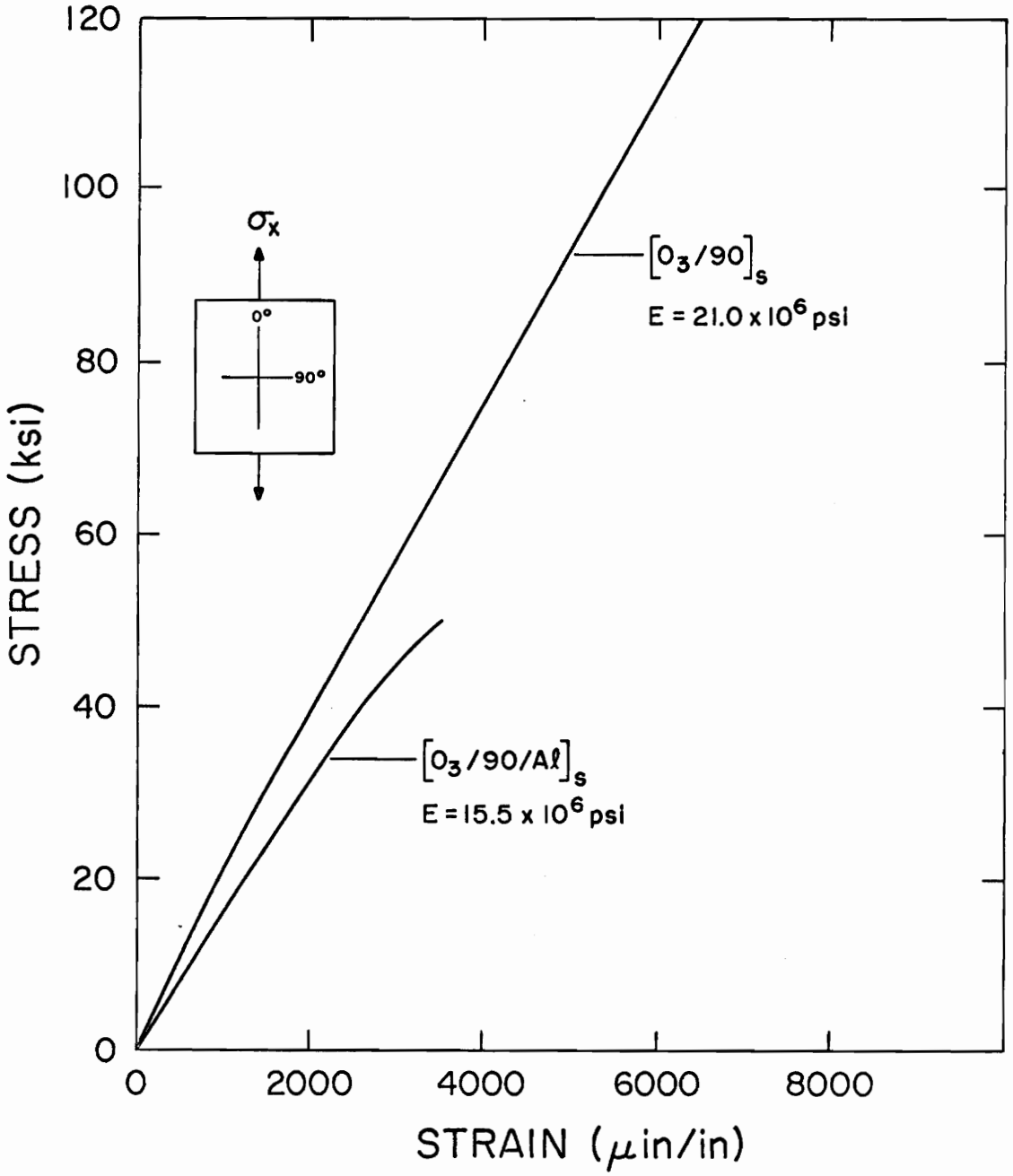

Figure 21. Comparison of Stress-Strain Diagrams for $[0_3/90]_s$ and $[0_3/90/A\ell]$ Laminates

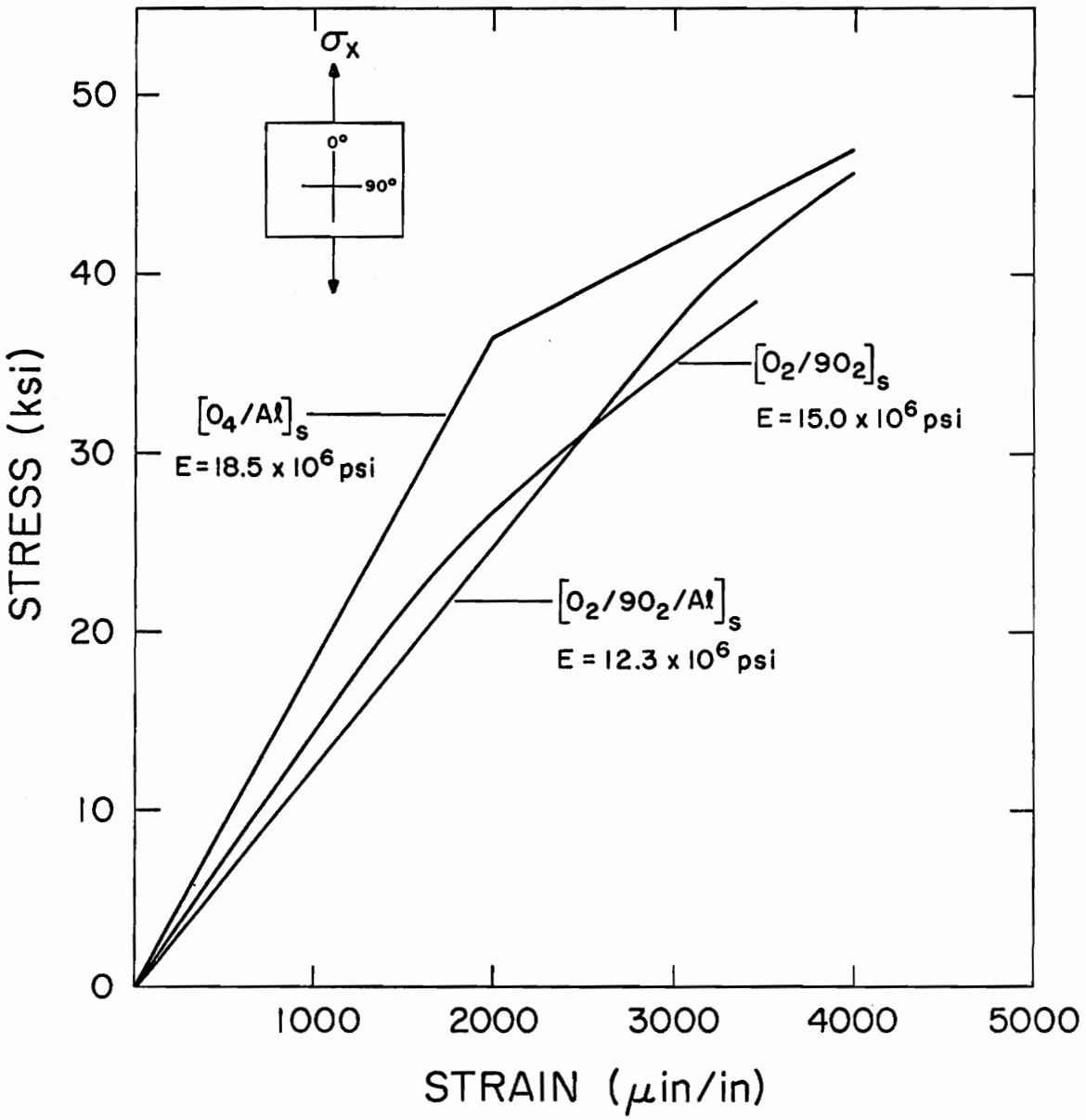

Figure 22. Comparison of Stress-Strain Diagrams for $[0_4/A\ell]_s$, $[0_2/90_2]_s$ and $[0_2/90_2/A\ell]_s$ Laminates

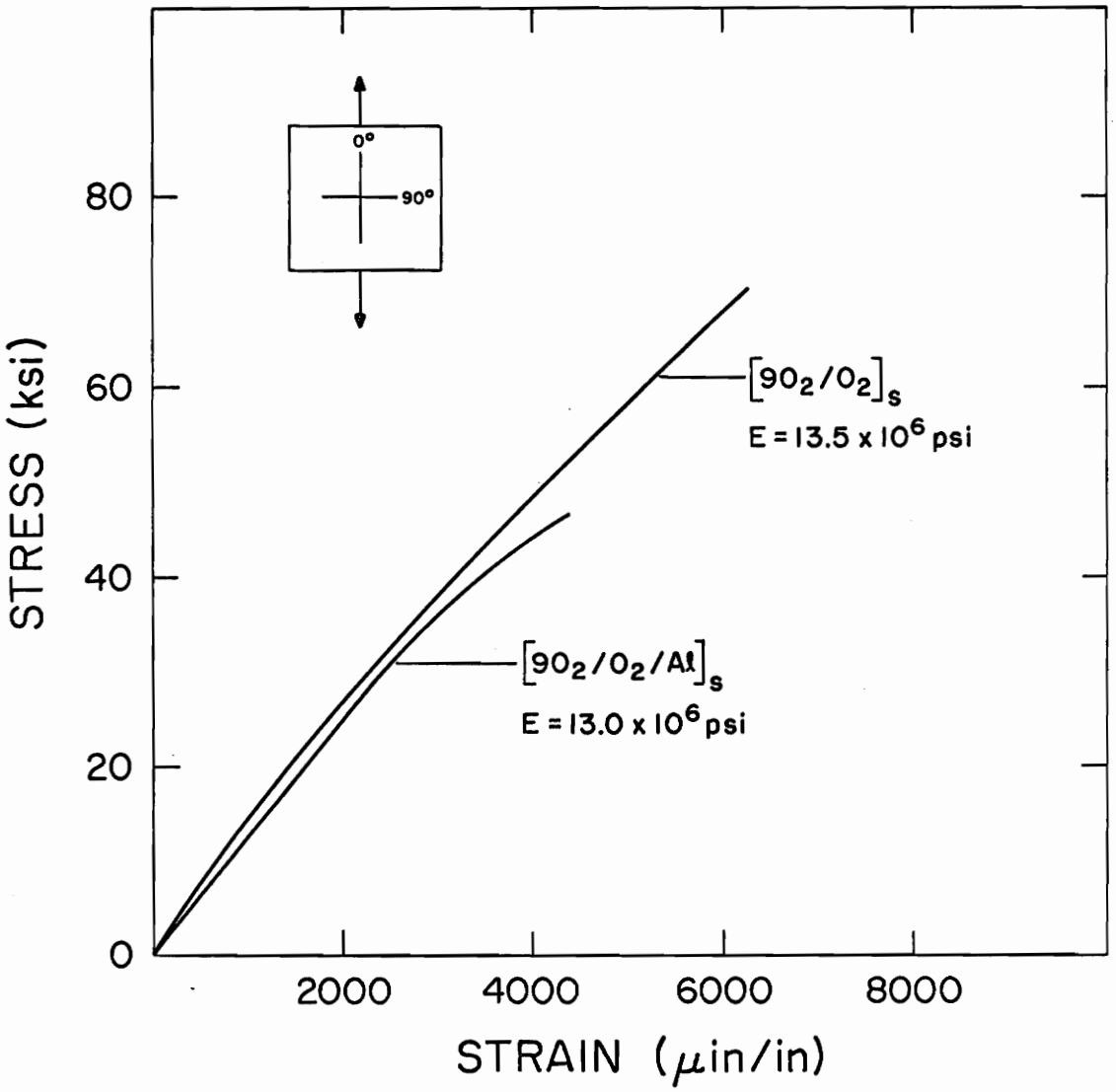

Figure 23. Comparison of Stress-Strain Diagrams for $[90_2/0_2]_s$ and $[90_2/0_2/Al]_s$ Laminates

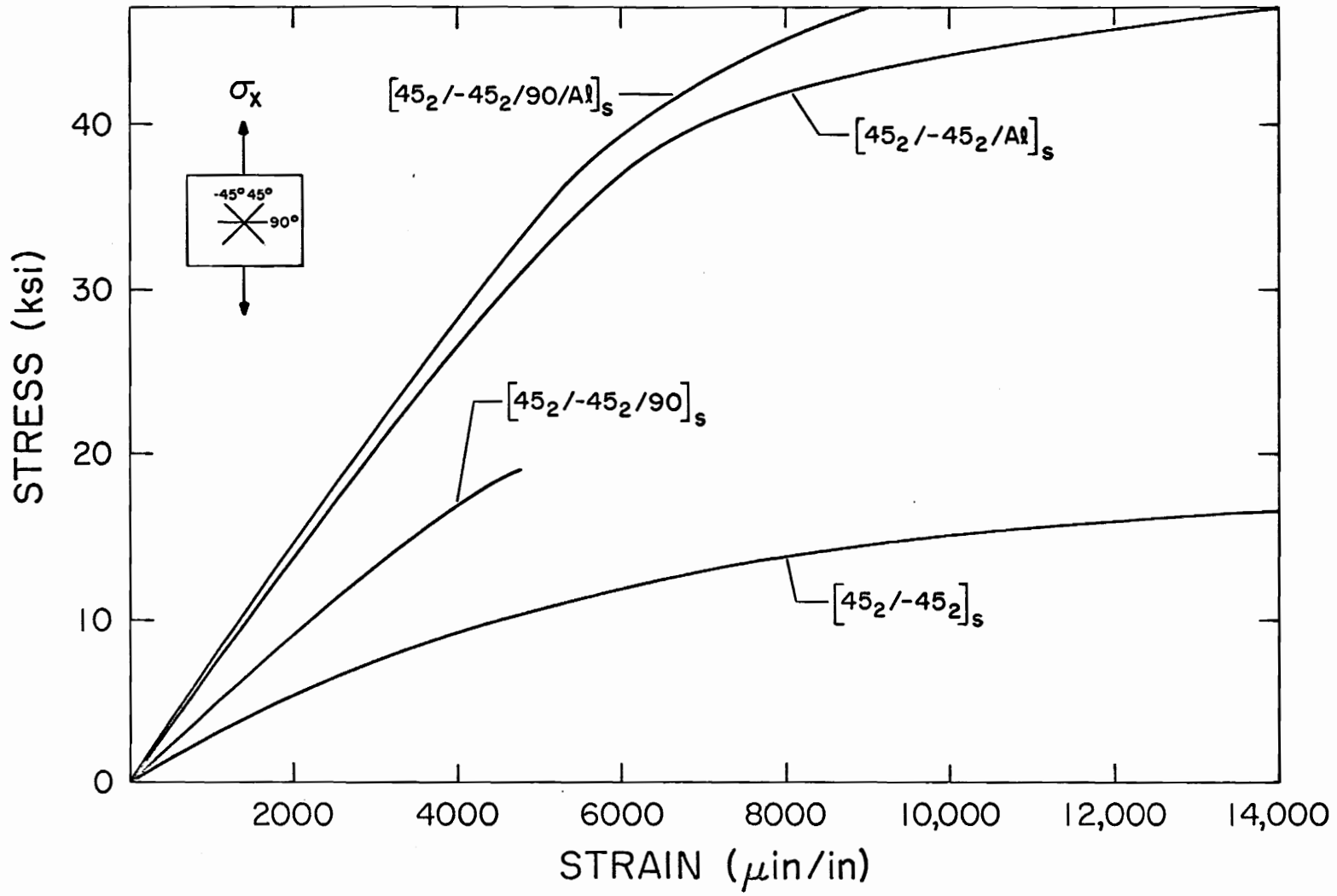

Figure 24. Comparison of Stress-Strain Diagrams for $[45_2/-45_2]_s$, $[45_2/-45_2/90]_s$, $[45_2/-45_2/A\ell]_s$ and $[45/-45_2/90/A\ell]$ Laminates.

REFERENCES

1. Kuebeler, G. C., Jordan, C. E., "Advanced Composites the New Diet Material for Structural Applications," Hercules Chemist, July, 1971.

2. Ashton, J. E., Halpin, J. C., Petit, P. H., Primer on Composite Material: Analysis. Technomic Publishing Co. Inc. Conn. 1969.

3. Sendeckyj, G. P., "A Brief Survey of Empirical Multiaxial Strength Criteria for Composites," Composite Material: Testing and Design (2nd Conference), ASTM STP 497, ASTM, 1972, pp. 41-51.

4. Sandhu, R. S., "A Survey of Failure Theories of Isotropic and Anisotropic Materials," Technical Report AFFDL-TR-72-71.

5. Herakovich, C. T., "Tensile Strength Behavior of Composite Reinforced Metals, Phase I Report: Boron/Epoxy Reinforced Metals," NASA Contract NASI-1-646-5, also. VPI & SU Report VPI-E-72-11, June, 1972.

6. Herakovich, C. T., Brooks, E. W. Jr., "Tensile Strength Behavior of Composite Reinforced Metals," Final Report, NASA Contract NASI-10646-5, also VPI & SU Report VPI-E-73-5, January 1973.

7. Pipes, R. B., Kaminski, B. E., Pagano, N. J., "The Influence of the Free Edge Upon the Strength of Angle-Ply Laminates," ASTM STP-521. Analysis of the Test Method for High Modulus Fibers and Composites, San Antonio, 1972.

8. Pagano, N. J. and Pipes, R. B., "The Influence of Stacking Sequence on Laminate Strength," Journal of Composite Materials, Vol. 5, 1971, p. 50.

9. Tsai, S. W. and Wu, E. M., "A general Theory of Strength for Anisotropic Materials," Journal of Composite Materials, Vo. 5 (Jan. 1971), p. 58.

10. Pipes, R. B. and Pagano, N. J., "Interlaminar Stresses in Composite Laminates Under Uniform Axial Extension," Journal of Composite Materials, Vol. 4, 1970, p. 538.

11. Pipes, R. B. and Pagano, N. J., "Boundary Layer Effects in Composite Laminates," ASCE Specialty Conference on "Selection, Design and Fabrication of Composites for Civil Engineering Structure," Nov. 13-14, 1972, Pittsburgh, Pa.

12. Kaminski, B. E., Lemon, G. H., and McKagne, E. L., "Development of Engineering Data for Advanced Composite Materials," Vol. 1, AFML-TR-70-108, (1972).

13. Reed, D. L., "Point Stress Laminate Analysis," SQ5, General Dynamics Report FZM-5494, April 1970.

VITA

The author was born on February 28th, 1948 in a small town near Canton, China. He lived his first thirteen years mostly in China and partly in Hong Kong. Upon emigrating to South America he graduated with honor from "Diez de Octubre" High School in Lima, Peru in 1966. He then came to the United States to start his studies of higher education at the Seattle Community College in 1967. In September, 1969 he transferred to the University of Washington, Seattle, Washington where he received his Bachelor of Science degree in Mechanical Engineering in 1972. He entered VPI & SU as a candidate toward the degree of Master of Science in Engineering Mechanics in September, 1972.

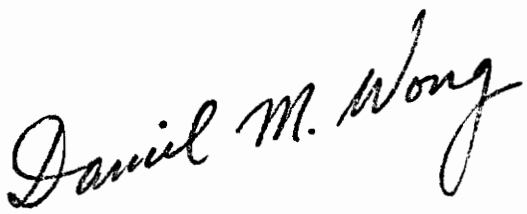

TENSILE BEHAVIOR OF ALUMINUM REINFORCED WITH ANGLE-PLY BORON/EPOXY LAMINATES

by

Daniel Ming-Fei Wong

(ABSTRACT)

An experimental investigation of the tensile behavior of aluminum reinforced with angle-ply boron/epoxy laminates was conducted. It is shown that the ultimate stresses of a wide variety of laminate configurations fall within a very narrow range of values. Some configurations of composite reinforced aluminum laminates exhibited higher ultimate stress values than the corresponding all composite laminates while other configurations exhibited lower ultimate stresses than the corresponding all composite laminates. Elastic moduli and Poisson ratios agreed quite well with predicted values but strength predictions were inconsistent.